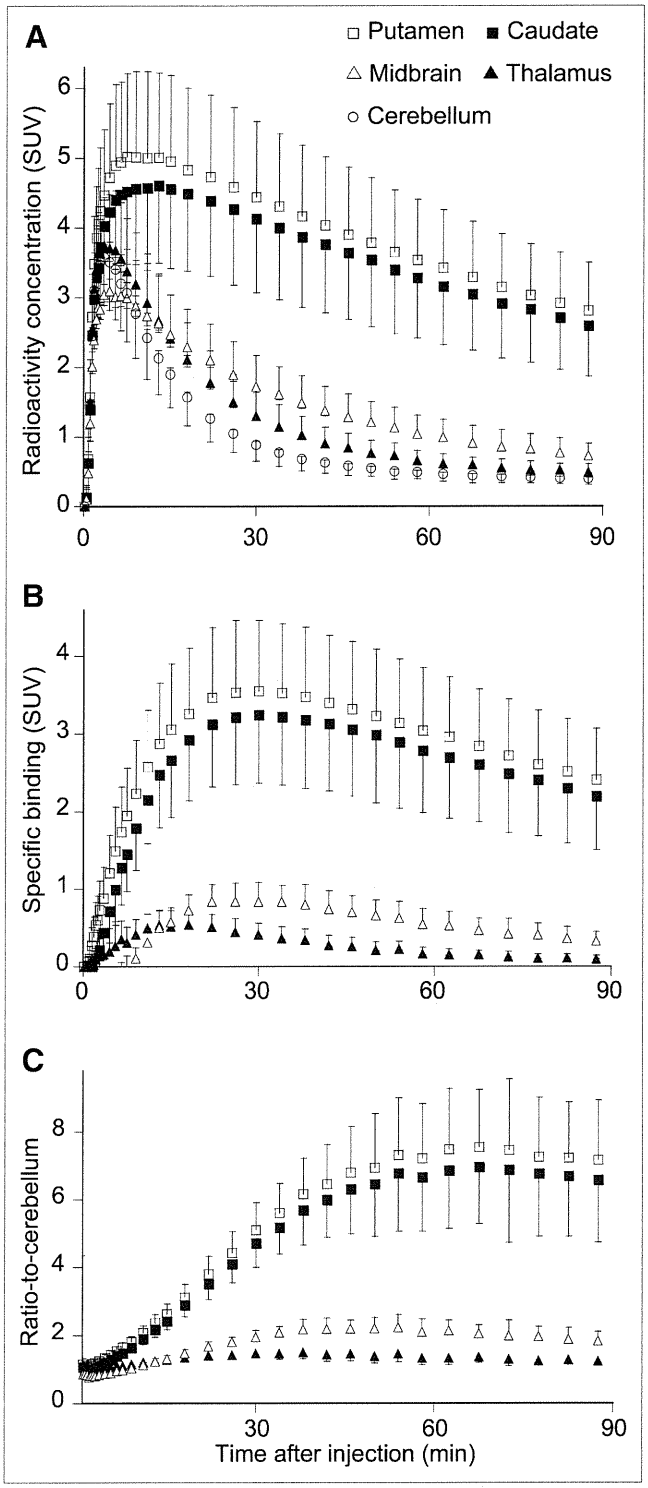

FIGURE 2. Average time course of radioactivity in brain regions after injection of ^{18}F-FE-PE2I. Time course for regional radioactivity (A), specific binding (B), and ratio to cerebellum (C). Data represent mean ± SD of all 10 subjects. SUV = standardized uptake value.

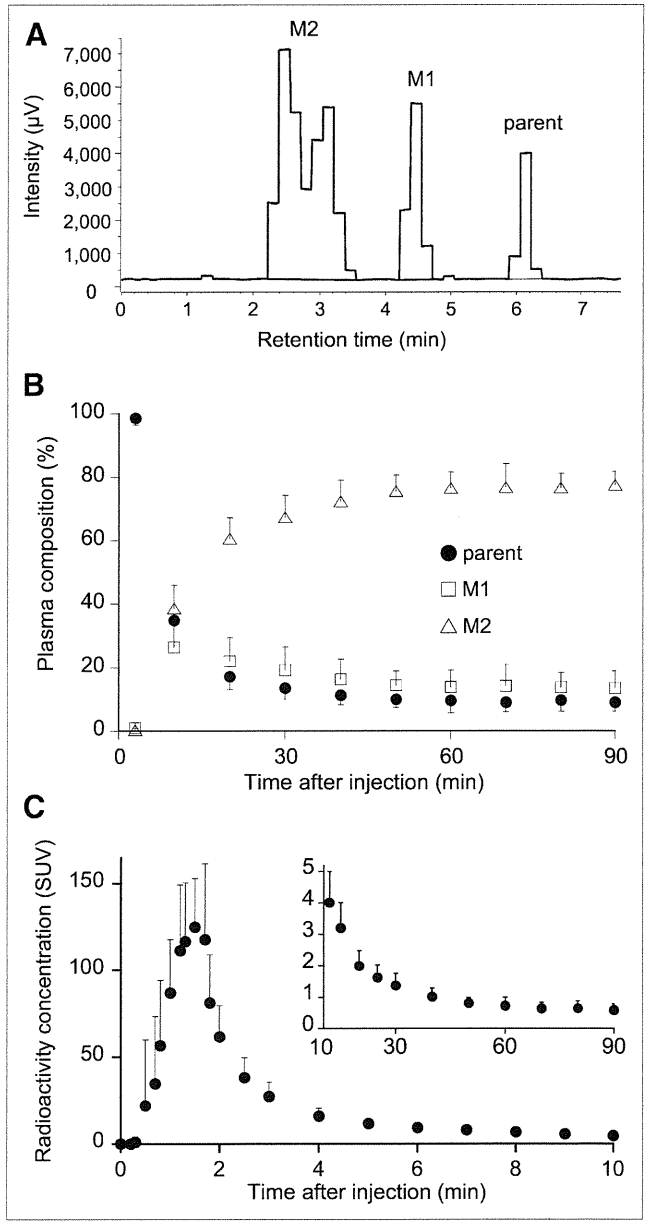

FIGURE 3. Concentration of ^{18}F-FE-PE2I and its composition in arterial plasma after injection of ^{18}F-FE-PE2I. (A) Representative radiochromatogram at 30 min after injection of ^{18}F-FE-PE2I. (B) Plasma composition of parent, M1, and M2. (C) Concentration of ^{18}F-FE-PE2I in plasma. Values from 0 to 10 and 10 to 90 min are shown in each graph with different ranges of *y*-axis. Data represent mean ± SD of all 10 subjects. SUV = standardized uptake value.

Quantification of DAT by Compartment Analysis

The 2-TCM provided significantly better fitting than the 1-TCM for all subjects in all regions. AIC of the 2-TCM was significantly lower than that of the 1-TCM in all regions in all subjects (paired *t* test, $P < 0.05$). The *F* test showed that the 2-TCM gave statistically better fittings than did the 1-TCM in all regions in all subjects ($F > 10.2$, $P < 0.001$). Thus, time–activity curves of all regions including the cerebellum were better described by the 2-TCM (Fig. 4).

The 2-TCM estimated K_1 and V_T with good identifiability (1.8% and 3.7%, respectively) (Table 1). BP_{ND} values estimated by the indirect kinetic method were approximately 4.0–4.5 in the putamen and caudate, approximately 0.5 in

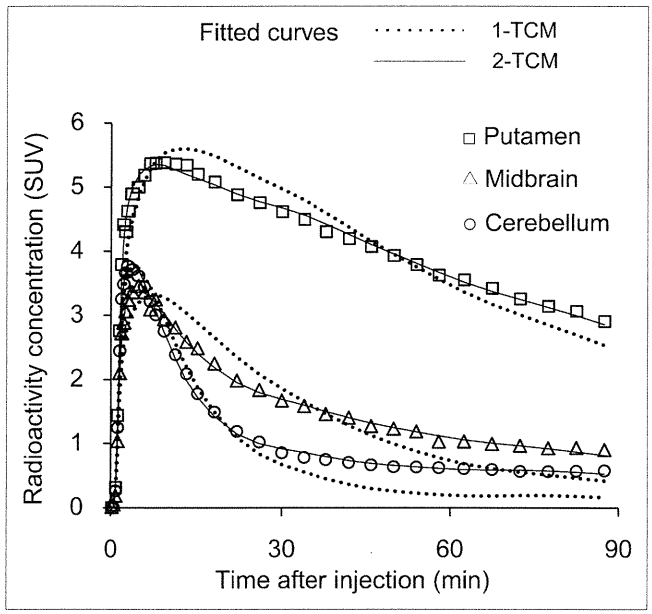

FIGURE 4. Representative fitted model curves of 1-TCM and 2-TCM. Time–activity curves in putamen, midbrain, and cerebellum were fitted to 1-TCM and 2-TCM using parent in plasma as input function. The 2-TCM (solid line) provided better fittings than 1-TCM (dotted line) for all 3 regions. SUV = standardized uptake value.

the midbrain, and approximately 0.2 in the thalamus (Table 2). As to the intersubject variability, the coefficients of variation (100 × SD/mean) of the BP_{ND} values were approximately 20%–25% in the putamen and caudate, approximately 30% in the midbrain, and approximately 60% in the thalamus.

Effects of Scan Length on Quantification of DAT

V_T values were stably estimated using the 2-TCM with 60-min or longer scan length. In the putamen and cerebellum, V_T values gradually increased with longer scan length (Figs. 5A and 5B). With a 60-min scan length, V_T values were approximately 94% and 90% of those with full scan length in the putamen and cerebellum, respectively, indicating that V_T values were stably estimated with a 60-min or longer scan length. Identifiability of V_T in the putamen improved over time, reaching approximately 2% at 90 min, whereas in the cerebellum, it remained at almost the same level (~6%) at a 60-min or longer scan length.

Effects of Adding Lipophilic Radiometabolite to Input Function on Quantification of DAT

To assess the effect of the lipophilic radiometabolite, we tested an alternative input function consisting of the concentration of the parent and M1, the lipophilic radiometabolite. Although the 2-TCM showed significantly better fitting than did the 1-TCM in the putamen, caudate, and midbrain based on AIC and the F test, V_T was not well identified by the 2-TCM in the thalamus in some subjects and in the cerebellum in most subjects. In the putamen, caudate, and midbrain, V_T values estimated using the alternative input function were approximately 30%–35% lower than V_T values estimated with the parent concentration in plasma as the input function (Supplemental Table 1; supplemental materials are available online only at http://jnm.snmjournals.org).

Quantification of DAT with SRTM Method

BP_{ND} values estimated by the SRTM method were approximately 3.6–4.0 in the putamen and caudate, approximately 0.6 in the midbrain, and approximately 0.3 in the thalamus (Table 2). Simple correlation analysis showed good correlation between BP_{ND} values estimated by the indirect kinetic method and by the SRTM method (r = 0.990, $P < 0.0001$) (Fig. 6), although there was significant difference between these values ($P = 0.0094$, paired t test). A Bland–Altman plot showed that the SRTM method underestimated BP_{ND} in the high-density regions and overestimated BP_{ND} in the low-density regions; however, the magnitude of the bias was small (~10% in the putamen, caudate, and midbrain) (Supplemental Fig. 1). The intersubject variability of BP_{ND} by the SRTM method was

TABLE 1
Kinetic Parameters by 2-TCM Using Parent as Input Function

Region	K_1 (mL·cm^{-3}·min^{-1})	k_2 (min^{-1})	k_3 (min^{-1})	k_4 (min^{-1})	K_1/k_2 (mL·cm^{-3})	k_3/k_4	V_T (mL·cm^{-3})	AIC
Putamen	0.292 ± 0.053 (1.7)	0.073 ± 0.022 (15)	0.133 ± 0.030 (21)	0.043 ± 0.007 (8.6)	4.25 ± 1.07 (13)	3.19 ± 0.97 (17)	17.3 ± 4.6 (2.0)	−43 ± 21
Caudate	0.248 ± 0.047 (1.7)	0.051 ± 0.022 (19)	0.110 ± 0.063 (38)	0.051 ± 0.014 (17)	5.71 ± 2.69 (18)	2.09 ± 0.93 (27)	16.2 ± 5.5 (2.6)	−38 ± 16
Midbrain	0.203 ± 0.044 (2.6)	0.095 ± 0.026 (13)	0.053 ± 0.028 (34)	0.042 ± 0.009 (22)	2.18 ± 0.37 (11)	1.29 ± 0.55 (18)	4.9 ± 1.1 (3.8)	20 ± 20
Thalamus	0.269 ± 0.042 (1.7)	0.123 ± 0.024 (6.0)	0.029 ± 0.018 (26)	0.041 ± 0.023 (23)	2.26 ± 0.55 (4.7)	0.71 ± 0.20 (12)	3.8 ± 0.8 (3.8)	10 ± 16
Cerebellum	0.265 ± 0.031 (1.2)	0.141 ± 0.025 (3.5)	0.013 ± 0.005 (23)	0.023 ± 0.013 (30)	1.94 ± 0.44 (2.6)	0.67 ± 0.32 (15)	3.2 ± 0.7 (6.3)	−4 ± 29

Values are mean ± SD (n = 10), with percentage SE (which is inversely related to identifiability of parameters) in parentheses.

TABLE 2
BP_{ND} Values by Indirect Kinetic and SRTM Methods

Region	BP_{ND}	
	Indirect kinetic	SRTM
Putamen	4.46 ± 0.95	4.05 ± 0.66
Caudate	4.06 ± 1.04	3.61 ± 0.67
Midbrain	0.55 ± 0.17	0.62 ± 0.13
Thalamus	0.20 ± 0.12	0.29 ± 0.08

Values are mean ± SD (n = 10).

approximately 15%–20% in the striatum and midbrain and approximately 30% in the thalamus, which were overall smaller than those by the indirect kinetic method. When BP_{ND} values estimated by the indirect kinetic method and by the SRTM method with 60-min data were compared with those estimated with 90-min data, good correlations were observed (r = 0.992 for the indirect kinetic method and 0.999 for the SRTM method, $P < 0.0001$ for both, Figs. 7A and 7B).

DISCUSSION

^{18}F-FE-PE2I is a promising radioligand for quantifying DAT in healthy humans. The kinetics of ^{18}F-FE-PE2I were well described by a standard 2-TCM using the parent radioligand in plasma as the input function. Although the radiometabolites of ^{18}F-FE-PE2I possibly have some effect on the radioactivity in the brain, the effect on the quantification was likely to be small. As a noninvasive quantification of DAT, the SRTM method was validated. The quantification was stable in both the striatum and the midbrain for both the indirect kinetic method with 2-TCM and the SRTM method with a scan duration of 60 min.

General kinetics of ^{18}F-FE-PE2I showed promising characteristics, including a high specific-to-nonspecific ratio and relatively fast washout. Uptake was high in the putamen and caudate, relatively low in the midbrain and thalamus, and lowest in the cerebellum. In all target regions, specific binding reached maximum values within the duration of PET data acquisition, and transient equilibrium was reached during this acquisition period. Uptake in the midbrain was visualized as 2 distinct regions. Given the selectivity of ^{18}F-FE-PE2I for DAT in the midbrain shown by a displacement study (*20*), we suppose that this uptake reflected DAT binding, not serotonin transporter binding.

Compartment model analysis showed that the kinetics of ^{18}F-FE-PE2I were well described by the 2-TCM using the parent radioligand in plasma as the input function. To estimate BP_{ND}, we applied the indirect kinetic method instead of directly using the ratio of k_3/k_4 values. The k_3/k_4 ratio theoretically equals BP_{ND}, but this estimate tends to be inaccurate because of data noise (*29*). We actually observed that these values showed poor identifiability and were not so reliably estimated (Table 1). Regional BP_{ND} values were

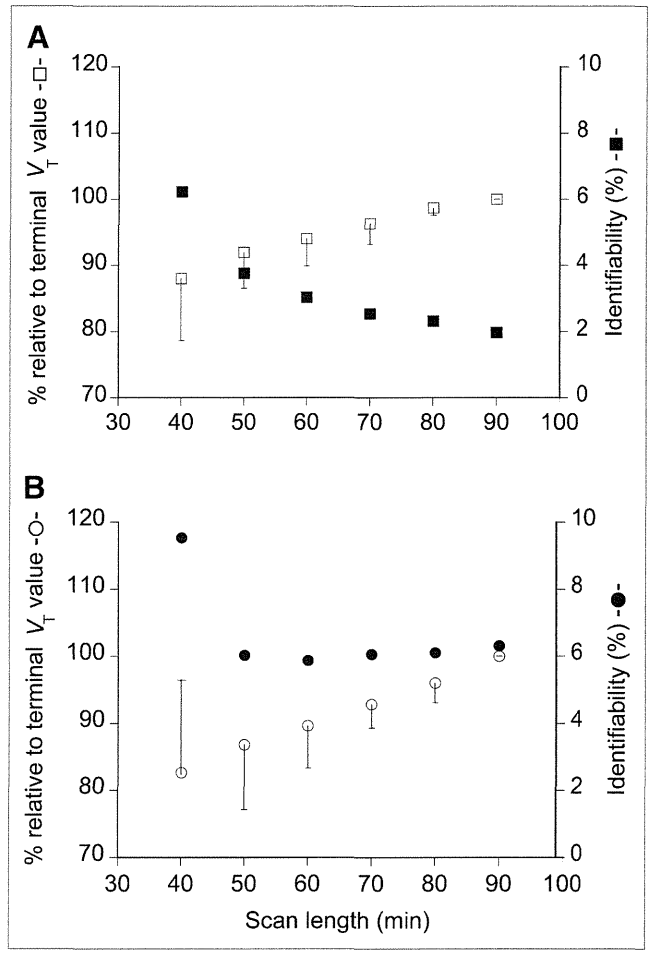

FIGURE 5. Value of V_T and identifiability as function of scan length. V_T and its corresponding SE (%) (SE (%)) were estimated in putamen (A) and cerebellum (B) with 2-TCM using parent as input function with truncating scan length from 90 to 40 min. V_T values are expressed as percentage of terminal value and plotted along left y-axis for putamen (□) and cerebellum (○). Corresponding SE (%), which is inversely related to identifiability, is plotted along right y-axis for putamen (■) and cerebellum (●). Error bar represents SD (n = 10).

in accordance with previous autoradiographic (*25*) and in vivo studies (*16,17*). As to intersubject variability, coefficients of variation of the BP_{ND} values were good in the putamen and caudate, acceptable in the midbrain, and poor in the thalamus. Because the BP_{ND} value in the midbrain was low (~13% of that in the striatum) in comparison with the results of autoradiography (~50% of that in the striatum) (*25*), the BP_{ND} values in the midbrain could be affected by the partial-volume effect. Similar results were obtained in nonhuman primates using high-resolution research tomography. BP_{ND} in the midbrain was approximately 15% of the values in the striatum (*21*).

Although radiometabolites of ^{18}F-FE-PE2I possibly have some effects on radioactivity in the brain, their effect on quantification was likely to be small. HPLC analysis detected 2 radiometabolites of ^{18}F-FE-PE2I in plasma,

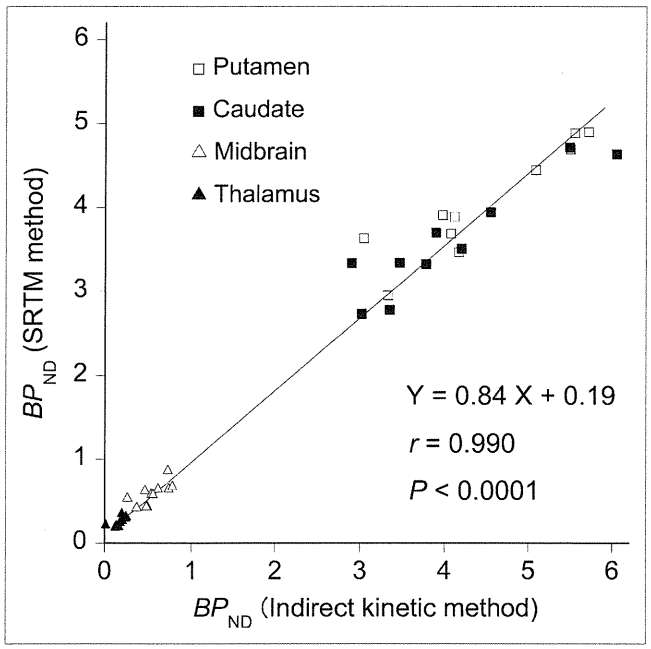

FIGURE 6. Correlation of BP_{ND} values estimated by indirect kinetic method using parent as input function and by SRTM method. BP_{ND} values showed significant correlation between 2 methods. Each data point represents BP_{ND} values in respective regions of each subject.

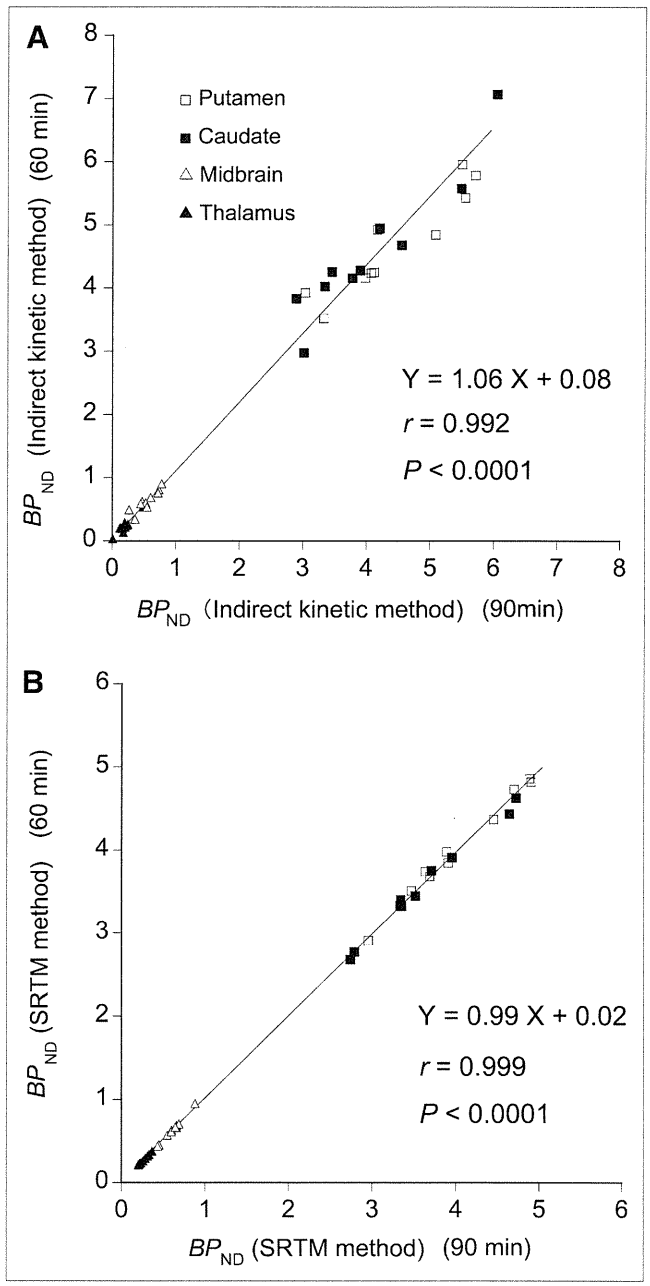

FIGURE 7. Correlation of BP_{ND} values estimated with 60- and 90-min data. (A) BP_{ND} values estimated by indirect kinetic method. (B) BP_{ND} values estimated by SRTM method. Significant correlations were observed in both methods between estimates with 60- and 90-min data.

one with intermediate (M1) and the other with lower (M2) lipophilicity. M1 and M2 would be 4-hydroxymethyl and 4-carboxyl analogs of ^{18}F-FE-PE2I, respectively, on the basis of the retention time of HPLC analysis, compared with the rat study (*19*). For clarity, in the following sentences, we refer to 4-hydroxymethyl and 4-carboxyl analogs of ^{11}C-PE2I as M1′ and M2′, respectively. In rats, M1′ entered the brain, accumulated in the striatum to a lesser extent than ^{11}C-PE2I, and metabolized to M2′, which accumulated in the brain. Mainly as a result of the accumulation of M2′, radioactivity in the cerebellum of rats did not decrease from 55 min to the end of the scan (120 min) (*19*). Whereas in the current study with ^{18}F-FE-PE2I, radioactivity in the cerebellum showed a gradual decrease to the end of the scan (90 min) (Fig. 2A), indicating that the amount of retention of radiometabolites in the brain in humans with ^{18}F-FE-PE2I was less than that in rats with ^{11}C-PE2I. This result was in accordance with the study in monkeys with ^{18}F-FE-PE2I (*21*).

The effects of radiometabolites on the quantification were small in the target and reference regions. To evaluate the effect of the possible accumulation of radiometabolites on the estimation of V_T, we performed a time–stability analysis of V_T. The increase in V_T with an increase in scan length could be interpreted as evidence for the accumulation of radiometabolites in the brain (*30*). In the current study, V_T values by the 2-TCM in the putamen and cerebellum with 60-min data were approximately 94% and 90% of terminal values with 90-min data (Fig. 6). This finding might indicate that V_T values were slightly affected by the radiometabolites, but the effects were relatively small.

To estimate the possible bias by the radiometabolites on V_T, we tried a combined input function of the parent and the radiometabolite M1 as previously performed by Varrone et al. in nonhuman primates using^{18} F-FE-PE2I (*21*). The main assumption of this approach is that the parent and the radiometabolite M1 would behave similarly and hence could be combined in a single input. With this approach,

the 2-TCM yielded approximately 30%–35% lower estimates of V_T values in the striatum and midbrain than with the 2-TCM using the parent as the input function. The decrease of V_T could be a possible maximum bias by the radiometabolites. However, the V_T values estimated by the 2-TCM using a summation of the parent and M1 as the input function were not well identified in some subjects in the thalamus and in most in the cerebellum. Because combining the parent and M1 as the input function did not improve the fitting, at least for these regions the assumption was not fully supported by the data. Identification of the radiometabolites of ^{18}F-FE-PE2I and assessment of their affinity for the DAT would be necessary to confirm or rule out the above assumption.

As a less noninvasive quantification of DAT without arterial blood data, BP_{ND} values were well estimated by the SRTM method using the cerebellum as the reference region. BP_{ND} values estimated by the SRTM method were well correlated with those estimated by the indirect kinetic method with the 2-TCM, which was not so much affected by radiometabolites as we discussed above. The SRTM method yielded slight underestimation and overestimation of BP_{ND} values in regions with high and low DAT densities, respectively, although the magnitude of the bias was small (~10% in the putamen, caudate, and midbrain). This bias seems to be an intrinsic limitation of the SRTM method because a similar phenomenon was observed in other ligands, including the serotonin 5-hydroxytryptamine-1A ligand ^{11}C-WAY-100653 (*31*), perhaps because of a violation of the assumptions of SRTM method. The intersubject variability of BP_{ND} values by the SRTM method were better than those by the indirect kinetic method with the 2-TCM, indicating that the SRTM method provided more precise estimation of BP_{ND} in all regions, including the midbrain.

Time–stability analysis indicated that 60-min scan duration is enough to estimate DAT binding with ^{18}F-FE-PE2I in humans. A recent study in nonhuman primates indicated that an approximately 60-min scan length was sufficient for the quantification of DAT with ^{18}F-FE-PE2I by the SRTM method (*32*). In the current study in humans, quantification was stable for both the indirect kinetic method and SRTM method with a scan duration of 60 min. Good correlations were observed between BP_{ND} values estimated with 60- and 90-min data for both the indirect kinetic method and the SRTM method.

^{18}F-FE-PE2I has many desirable characteristics among DAT ligands available for human imaging. High affinity and high selectivity for DAT allowed reliable quantification of specific binding not only in the striatum but also in the midbrain. Because of the faster kinetics even in high-density regions (i.e., the striatum), quantification with a shorter time (60 min) was possible, and the SRTM method yielded less biased BP_{ND} in the striatum than ^{11}C-PE2I. In addition, labeling with ^{18}F, which has a longer half-life than ^{11}C (110 vs. 20 min), allows distribution of the radioligand to PET centers without a cyclotron.

^{18}F-labeled DAT ligands previously reported in humans include ^{18}F-FPCIT (*12*), ^{18}F-CFT (^{18}F-WIN35,428) (*11*), and ^{18}F-FECNT (*13*). All of these ligands have a high affinity for DAT, and the maximum striatum-to-cerebellum ratios have been reported to be approximately 3.5–9.0. The possible advantage of ^{18}F-FPCIT and ^{18}F-FECNT could be the absence of potentially BBB-permeable radiometabolites. However, the disadvantage of those ligands was that the kinetics are slow, requiring over 90 min to reach peak brain uptake in the striatum. Among ^{18}F-labeled DAT ligands, ^{18}F-FE-PE2I has a relatively high striatum-to-cerebellum ratio (~7.0) and obviously the fastest kinetics.

One of the 2 limitations of the current study is the absence of the measurement of the free fraction in plasma, which would enable us to measure DAT density more accurately. Another limitation is the absence of an animal ex vivo study using ^{18}F-FE-PE2I to examine the BBB permeability and affinity for DAT of the radiometabolites. These issues should be explored in future studies.

CONCLUSION

^{18}F-FE-PE2I is a promising radioligand for quantifying DAT in healthy humans. The kinetics of ^{18}F-FE-PE2I were well described by a standard 2-TCM using the parent radioligand in plasma as the input function. Although radiometabolites of ^{18}F-FE-PE2I possibly have some effect on the radioactivity in the brain, their effect on quantification was likely to be small. As a noninvasive quantification of DAT, the SRTM method was validated. The quantification was stable in both the striatum and the midbrain for both the indirect kinetic method with 2-TCM and the SRTM method with a scan duration of 60 min, although the SRTM method yielded a slight underestimation and overestimation of BP_{ND} values in regions with high and low DAT densities, respectively. If no major differences in metabolism between patients and controls are present in clinical studies, noninvasive estimation of BP_{ND} by the SRTM method with a 60-min scan will be sufficiently accurate for DAT quantification.

DISCLOSURE STATEMENT

The costs of publication of this article were defrayed in part by the payment of page charges. Therefore, and solely to indicate this fact, this article is hereby marked "advertisement" in accordance with 18 USC section 1734.

ACKNOWLEDGMENTS

We thank Katsuyuki Tanimoto, Takahiro Shiraishi, and Takehito Ito for their assistance in performing PET experiments and Izumi Izumida and Kazuko Suzuki for their help as clinical research coordinators. This study was supported by a grant-in-aid for Molecular Imaging Program from the Ministry of Education, Culture, Sports, Science and Technology and by a Health Labour Sciences Research

grant from the Ministry of Health, Labour and Welfare, Japanese government. No other potential conflict of interest relevant to this article was reported.

REFERENCES

1. Hurley MJ, Mash DC, Jenner P. Markers for dopaminergic neurotransmission in the cerebellum in normal individuals and patients with Parkinson's disease examined by RT-PCR. *Eur J Neurosci.* 2003;18:2668–2672.
2. Ginovart N, Lundin A, Farde L, et al. PET study of the pre- and post-synaptic dopaminergic markers for the neurodegenerative process in Huntington's disease. *Brain.* 1997;120:503–514.
3. Jucaite A, Fernell E, Halldin C, Forssberg H, Farde L. Reduced midbrain dopamine transporter binding in male adolescents with attention-deficit/hyperactivity disorder: association between striatal dopamine markers and motor hyperactivity. *Biol Psychiatry.* 2005;57:229–238.
4. Nakamura K, Sekine Y, Ouchi Y, et al. Brain serotonin and dopamine transporter bindings in adults with high-functioning autism. *Arch Gen Psychiatry.* 2010;67:59–68.
5. Arakawa R, Ichimiya T, Ito H, et al. Increase in thalamic binding of [^{11}C]PE2I in patients with schizophrenia: a positron emission tomography study of dopamine transporter. *J Psychiatr Res.* 2009;43:1219–1223.
6. Fowler JS, Volkow ND, Wolf AP, et al. Mapping cocaine binding sites in human and baboon brain in vivo. *Synapse.* 1989;4:371–377.
7. Wong DF, Yung B, Dannals RF, et al. In vivo imaging of baboon and human dopamine transporters by positron emission tomography using [^{11}C]WIN 35,428. *Synapse.* 1993;15:130–142.
8. Farde L, Halldin C, Muller L, Suhara T, Karlsson P, Hall H. PET study of [^{11}C] beta-CIT binding to monoamine transporters in the monkey and human brain. *Synapse.* 1994;16:93–103.
9. Ding YS, Fowler JS, Volkow ND, et al. Pharmacokinetics and in vivo specificity of [^{11}C]dl-threo-methylphenidate for the presynaptic dopaminergic neuron. *Synapse.* 1994;18:152–160.
10. Fischman AJ, Bonab AA, Babich JW, et al. [^{11}C, ^{127}I] Altropane: a highly selective ligand for PET imaging of dopamine transporter sites. *Synapse.* 2001;39:332–342.
11. Laakso A, Bergman J, Haaparanta M, Vilkman H, Solin O, Hietala J. [^{18}F]CFT ([^{18}F]WIN 35,428], a radioligand to study the dopamine transporter with PET: characterization in human subjects. *Synapse.* 1998;28:244–250.
12. Kazumata K, Dhawan V, Chaly T, et al. Dopamine transporter imaging with fluorine-18-FPCIT and PET. *J Nucl Med.* 1998;39:1521–1530.
13. Davis MR, Votaw JR, Bremner JD, et al. Initial human PET imaging studies with the dopamine transporter ligand ^{18}F-FECNT. *J Nucl Med.* 2003;44:855–861.
14. Emond P, Garreau L, Chalon S, et al. Synthesis and ligand binding of nortropane derivatives: N-substituted 2beta-carbomethoxy-3beta-(4′-iodophenyl)nortropane and N-(3-iodoprop-(2E)-enyl)-2beta-carbomethoxy-3beta-(3′,4′-disubstituted phenyl)nortropane: new high-affinity and selective compounds for the dopamine transporter. *J Med Chem.* 1997;40:1366–1372.
15. Halldin C, Erixon-Lindroth N, Pauli S, et al. [^{11}C]PE2I: a highly selective radioligand for PET examination of the dopamine transporter in monkey and human brain. *Eur J Nucl Med Mol Imaging.* 2003;30:1220–1230.
16. Jucaite A, Odano I, Olsson H, Pauli S, Halldin C, Farde L. Quantitative analyses of regional [^{11}C]PE2I binding to the dopamine transporter in the human brain: a PET study. *Eur J Nucl Med Mol Imaging.* 2006;33:657–668.
17. Hirvonen J, Johansson J, Teras M, et al. Measurement of striatal and extrastriatal dopamine transporter binding with high-resolution PET and [^{11}C]PE2I: quantitative modeling and test-retest reproducibility. *J Cereb Blood Flow Metab.* 2008;28:1059–1069.
18. Seki C, Ito H, Ichimiya T, et al. Quantitative analysis of dopamine transporters in human brain using [^{11}C]PE2I and positron emission tomography: evaluation of reference tissue models. *Ann Nucl Med.* 2010;24:249–260.
19. Shetty HU, Zoghbi SS, Liow JS, et al. Identification and regional distribution in rat brain of radiometabolites of the dopamine transporter PET radioligand [^{11}C] PE2I. *Eur J Nucl Med Mol Imaging.* 2007;34:667–678.
20. Varrone A, Steiger C, Schou M, et al. In vitro autoradiography and in vivo evaluation in cynomolgus monkey of [^{18}F]FE-PE2I, a new dopamine transporter PET radioligand. *Synapse.* 2009;63:871–880.
21. Varrone A, Toth M, Steiger C, et al. Kinetic analysis and quantification of the dopamine transporter in the nonhuman primate brain with ^{11}C-PE2I and ^{18}F-FE-PE2I. *J Nucl Med.* 2011;52:132–139.
22. Schou M, Steiger C, Varrone A, Guilloteau D, Halldin C. Synthesis, radiolabeling and preliminary in vivo evaluation of [^{18}F]FE-PE2I, a new probe for the dopamine transporter. *Bioorg Med Chem Lett.* 2009;19:4843–4845.
23. Innis RB, Cunningham VJ, Delforge J, et al. Consensus nomenclature for in vivo imaging of reversibly binding radioligands. *J Cereb Blood Flow Metab.* 2007;27: 1533–1539.
24. Leenders KL, Perani D, Lammertsma AA, et al. Cerebral blood flow, blood volume and oxygen utilization: normal values and effect of age. *Brain.* 1990; 113:27–47.
25. Hall H, Halldin C, Guilloteau D, et al. Visualization of the dopamine transporter in the human brain postmortem with the new selective ligand [^{125}I]PE2I. *Neuroimage.* 1999;9:108–116.
26. Lammertsma AA, Hume SP. Simplified reference tissue model for PET receptor studies. *Neuroimage.* 1996;4:153–158.
27. Akaike H. A new look at the statistical model identification. *IEEE Trans Automat Contr.* 1974;19:716–723.
28. Carson R. Parameters estimation in positron emission tomography. In: Phelps M, Mazziotta J, Schelbert H, eds. *Positron Emission Tomography Principle Applications for the Brain and the Heart.* New York, NY: Raven Press; 1986:347–390.
29. Seneca N, Skinbjerg M, Zoghbi SS, et al. Kinetic brain analysis and whole-body imaging in monkey of [^{11}C]MNPA: a dopamine agonist radioligand. *Synapse.* 2008;62:700–709.
30. Terry G, Liow JS, Chernet E, et al. Positron emission tomography imaging using an inverse agonist radioligand to assess cannabinoid CB1 receptors in rodents. *Neuroimage.* 2008;41:690–698.
31. Parsey RV, Slifstein M, Hwang DR, et al. Validation and reproducibility of measurement of 5-HT1A receptor parameters with [carbonyl-^{11}C]WAY-100635 in humans: comparison of arterial and reference tisssue input functions. *J Cereb Blood Flow Metab.* 2000;20:1111–1133.
32. Varrone A, Gulyas B, Takano A, Stabin MG, Jonsson C, Halldin C. Simplified quantification and whole-body distribution of [^{18}F]FE-PE2I in nonhuman primates: prediction for human studies. *Nucl Med Biol.* 2012;39:295–303.

PLOS ONE

Effects of Dopamine D_2 Receptor Partial Agonist Antipsychotic Aripiprazole on Dopamine Synthesis in Human Brain Measured by PET with L-[β-^{11}C]DOPA

Hiroshi Ito*, Harumasa Takano, Ryosuke Arakawa, Hidehiko Takahashi, Fumitoshi Kodaka, Keisuke Takahata, Tsuyoshi Nogami, Masayuki Suzuki, Tetsuya Suhara

Molecular Imaging Center, National Institute of Radiological Sciences, Chiba, Japan

Abstract

Dopamine D_2 receptor partial agonist antipsychotic drugs can modulate dopaminergic neurotransmission as functional agonists or functional antagonists. The effects of antipsychotics on presynaptic dopaminergic functions, such as dopamine synthesis capacity, might also be related to their therapeutic efficacy. Positron emission tomography (PET) was used to examine the effects of the partial agonist antipsychotic drug aripiprazole on presynaptic dopamine synthesis in relation to dopamine D_2 receptor occupancy and the resulting changes in dopamine synthesis capacity in healthy men. On separate days, PET studies with [^{11}C]raclopride and L-[β-^{11}C]DOPA were performed under resting condition and with single doses of aripiprazole given orally. Occupancy of dopamine D_2 receptors corresponded to the doses of aripiprazole, but the changes in dopamine synthesis capacity were not significant, nor was the relation between dopamine D_2 receptor occupancy and these changes. A significant negative correlation was observed between baseline dopamine synthesis capacity and changes in dopamine synthesis capacity by aripiprazole, indicating that this antipsychotic appears to stabilize dopamine synthesis capacity. The therapeutic effects of aripiprazole in schizophrenia might be related to such stabilizing effects on dopaminergic neurotransmission responsivity.

Citation: Ito H, Takano H, Arakawa R, Takahashi H, Kodaka F, et al. (2012) Effects of Dopamine D_2 Receptor Partial Agonist Antipsychotic Aripiprazole on Dopamine Synthesis in Human Brain Measured by PET with L-[β-^{11}C]DOPA. PLoS ONE 7(9): e46488. doi:10.1371/journal.pone.0046488

Editor: Kenji Hashimoto, Chiba University Center for Forensic Mental Health, Japan

Received May 31, 2012; **Accepted** September 5, 2012; **Published** September 28, 2012

Funding: This study was supported in part by a Grant-in-Aid for Molecular Imaging Program from the Ministry of Education, Culture, Sports, Science and Technology (MEXT), Japanese Government, a Grant-in-Aid for Scientific Research (C) (No. 21591587) from the Japan Society for the Promotion of Science, and a grant from the National Institute of Radiological Sciences. The funders had no role in study design, data collection and analysis, decision to publish, or preparation of the manuscript.

Competing Interests: The authors have declared that no competing interests exist.

* E-mail: hito@nirs.go.jp

Introduction

Effects of antipsychotic drugs with antagonistic property mediated by blockade of postsynaptic dopamine D_2 receptors can be evaluated by positron emission tomography (PET) studies for determining the occupancy of dopamine D_2 receptors in schizophrenia patients treated with first-generation antipsychotics, e.g., haloperidol [1,2] and second-generation antipsychotics, e.g., risperidone [3], antagonists of dopamine D_2 receptors. Recently, a new atypical antipsychotic drug acting as a partial agonist of dopamine D_2 receptors, aripiprazole, has been widely used for the treatment of schizophrenia [4]. Partial agonists of dopamine D_2 receptors can modulate the dopaminergic neurotransmission as functional agonists or functional antagonists [5].

Effects of antipsychotics on presynaptic dopaminergic functions, e.g., dopamine synthesis capacity, might also be related to their therapeutic effects. The regional activity of aromatic L-amino acid decarboxylase (AADC) in brain, indicating dopamine synthesis capacity, can be estimated using radiolabeled L-DOPA [6]. Animal studies showed significant increases and decreases in dopamine synthesis capacities by antagonists and agonists of dopamine D_2 receptors using [^{3}H]DOPA, L-[β-^{11}C]DOPA, and 6-[^{18}F]fluoro-L-DOPA, respectively [7–9]. These findings suggest that changes in presynaptic dopamine synthesis capacity might be caused by the pharmacological effects on dopaminergic autoreceptors [10]. On the other hand, an increase in dopamine synthesis capacity by administration of the partial agonist antipsychotic aripiprazole was observed in animal studies by measuring DOPA accumulation [11].

Effects of antipsychotics with antagonistic property on dopamine synthesis capacity have been studied in brains of human subjects. The acute administration of the antipsychotic drug haloperidol and the use of PET with 6-[^{18}F]fluoro-L-DOPA revealed a significant increase in dopamine synthesis capacity in healthy human subjects [12]. In contrast, in schizophrenia patients, a significant decrease in dopamine synthesis capacity after chronic administration of haloperidol was observed with PET and 6-[^{18}F]fluoro-L-DOPA [13]. Recently, we found that the antipsychotic drug risperidone could be considered to stabilize dopamine synthesis capacity in healthy human subjects, indicating that the therapeutic effects of risperidone in schizophrenia might be related to the stabilizing effects on dopaminergic neurotransmission responsivity [14]. However, the effects of the partial agonist antipsychotic aripiprazole on dopamine synthesis capacity have not yet been investigated in human subjects.

In the present study, dopamine D_2 receptor bindings and dopamine synthesis capacities at resting condition and after oral

administration of a single dose of aripiprazole were measured in the same human subjects by PET with [^{11}C]raclopride and L-[β-^{11}C]DOPA, respectively, to determine changes in dopamine synthesis capacity by this antipsychotic in relation to the occupancy of dopamine D_2 receptors. Similar experimental protocol as previous our work with risperidone was used, and results were compared [14].

Results

The occupancies of dopamine D_2 receptors for each dose of aripiprazole as measured by PET with [^{11}C]raclopride ranged from 53% to 79% in the caudate and from 51% to 77% in the putamen (Table 1). Typical images of [^{11}C]raclopride for baseline and drug challenge studies are shown in Fig. 1. Reduced uptake of [^{11}C]raclopride in the striatum was observed after oral administration of aripiprazole.

The plasma concentrations of aripiprazole during [^{11}C]raclopride and L-[β-^{11}C]DOPA PET studies, averaged between the start and end of each scanning, were 12.0±2.1 ng/mL (mean ± SD) and 10.4±1.5 ng/mL for 3 mg of oral administration dose of aripiprazole, 29.0±2.1 ng/mL and 25.6±2.1 ng/mL for 6 mg, and 39.6–40.4 ng/mL and 38.2–39.7 ng/mL for 9 mg, respectively. The plasma concentrations of dehydroaripiprazole during [^{11}C]raclopride and L-[β-^{11}C]DOPA PET studies were 0.4±0.2 ng/mL (mean ± SD) and 0.5±0.2 ng/mL for 3 mg of oral administration dose of aripiprazole, 0.9±0.3 ng/mL and 1.1±0.4 ng/mL for 6 mg, and 1.1–1.6 ng/mL and 1.4–2.4 ng/mL for 9 mg, respectively.

The uptake rate constants k_i of L-[β-^{11}C]DOPA in the caudate and putamen, indicating the dopamine synthesis capacity for baseline and drug challenge studies, are shown in Table 2. No significant differences in k_i were observed between the two studies (paired t-test). Typical images of L-[β-^{11}C]DOPA for baseline study are shown in Fig. 2. Weighted sums of the natural neutral amino acids (NAAs) concentrations in plasma were 1170±142 nmol/mL for the baseline study and 1122±154 nmol/mL (mean ± SD) for the drug challenge study. The values showed no significant differences between the two studies (paired t-test).

Fig. 3 shows the relations between dopamine D_2 receptor occupancy and percentage changes in k_i by the drug challenge. There were no significant correlations. No dose dependency was observed in percentage changes in k_i by the drug challenge. The relations between k_i in the baseline study and percentage change in k_i by the drug challenge for each administration dose of aripiprazole are shown in Fig. 4. Significant negative correlations were observed among all administration dose (caudate: $P = 0.005$, putamen: $P = 0.027$).

Table 1. Dose of aripiprazole and ranges of occupancy of dopamine D_2 receptors.

Dose of aripiprazole	Occupancy (%)	
(mg)	Caudate	Putamen
3	53–61%	51–58%
	(57±4%)	(55±2%)
6	70–77%	66–72%
	(73±3%)	(69±3%)
9	77–79%	75–77%

(mean ± SD).
doi:10.1371/journal.pone.0046488.t001

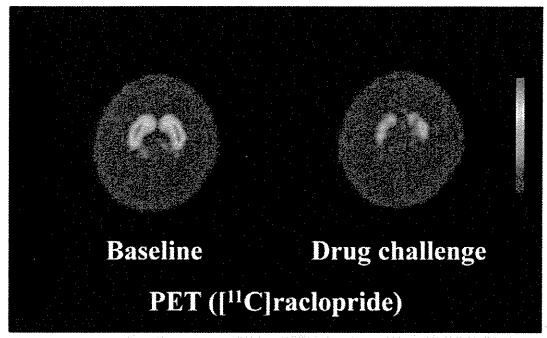

Figure 1. Typical PET summation images of frames between 32–60 min after intravenous injection of [^{11}C]raclopride for baseline and drug challenge (6 mg of aripiprazole) studies. The sections are transaxial at the level of putamen.
doi:10.1371/journal.pone.0046488.g001

Discussion

The present study was performed using similar experimental protocol as previous our work with the antipsychotic risperidone, an antagonist for dopamine D_2 receptors [14]. The effects of antipsychotics on presynaptic dopamine synthesis might be due to pharmacological action on dopaminergic autoreceptors [10] and by neural network regulation. While occupancy of dopamine D_2 receptors corresponding to the dose of aripiprazole was observed [15–18], the current study showed no significant changes in dopamine synthesis capacity by the administration of aripiprazole. There were also no significant correlations between the occupancy of dopamine D_2 receptors and changes in dopamine synthesis capacity by aripiprazole. These findings are similar to our previous observation in healthy human subjects using risperidone [14]. To our knowledge, this is the first study to investigate the effects of aripiprazole on dopamine synthesis capacity in humans using PET. Significant increases and decreases in dopamine synthesis capacities by antagonists and agonists, respectively, of dopamine D_2 receptors were observed in animal studies [7–9], indicating that pharmacological effects on dopaminergic autoreceptors and the neural network might cause changes in presynaptic dopamine synthesis capacity [10]. An increase in dopamine synthesis capacity by aripiprazole was observed in animal studies [11], although partial agonists for dopamine D_2 receptors might reduce presynaptic activity through feedback regulation [5,19]. However, no significant changes in dopamine synthesis capacity by a single administration of an antagonist or a partial agonist were observed

Table 2. Dopamine synthesis capacity k_i of both baseline and drug challenge studies.

	Caudate	Putamen
Baseline	0.0114±0.0022	0.0134±0.0014
Drug challenge	0.0111±0.0016	0.0136±0.0014

Values are mean ± SD.
Unit is min^{-1}.
No significant differences in k_i are observed between the two studies (paired t-test).
doi:10.1371/journal.pone.0046488.t002

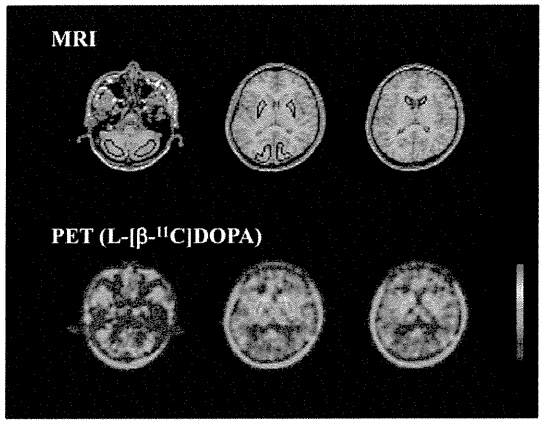

Figure 2. Regions of interest (ROIs) drawn on coregistered MR images. ROIs are defined for the cerebellar cortex, putamen, caudate head, and occipital cortex. Typical PET summation images of frames between 29–89 min after intravenous injection of L-[β-^{11}C]DOPA for baseline study are also shown.
doi:10.1371/journal.pone.0046488.g002

in healthy human subjects. The inconsistency of changes in dopamine synthesis capacity between the present study and previous animal studies might be due to differences in administration dose and way of aripiprazole.

In the present study, significant negative correlations were observed between baseline dopamine synthesis capacity and the percentage changes in dopamine synthesis capacity by aripiprazole. This indicates that aripiprazole administration causes either increase or decrease in dopamine synthesis capacity in subjects with low or high baseline dopamine synthesis capacity, respectively, and the degrees of increase and decrease in dopamine synthesis capacity depend on the baseline dopamine synthesis capacities. These findings are similar to our previous observation in healthy human subjects using the antagonist antipsychotic risperidone [14] and a previous report using the antagonist antipsychotic haloperidol [20]. In addition, the coefficients of variation of dopamine synthesis capacity were smaller in studies with the administration of aripiprazole than in baseline studies, the same as with risperidone [14]. These results indicate that the partial agonist antipsychotic aripiprazole can be assumed to stabilize dopamine synthesis capacity in the same way as antipsychotic drugs with antagonistic property. These also indicate that there are two groups in the healthy subjects with relatively high and low baseline dopamine synthesis capacities, however, we could not find any differences between the two groups. Although stabilizing effect of antipsychotic drugs on dopamine synthesis capacity were observed both in the antagonist and partial agonist antipsychotic drugs, its mechanism would be unknown. An abnormal responsivity in both phasic and tonic dopamine release, which might be related to the modulation of dopaminergic neurotransmission, has been considered in the pathophysiology of schizophrenia [21]. The therapeutic effects of aripiprazole might be related to stabilizing effects on such dopaminergic responsivity. It has also been reported that aripiprazole suppressed phasic dopamine release in methamphetamine-sensitized rat [22]. Although the occupancy of dopamine D_2 receptors ranged from about 50% to 80% in the present study, there might be some kind of threshold of occupancy by aripiprazole for the stabilizing effect of dopamine synthesis capacity to emerge. Further investigations about such threshold should be considered.

The occupancy of dopamine D_2 receptors in this study might be relatively lower than in previous reports regarding drug challenge studies being performed after daily administration of aripiprazole for more than ten days [15,18]. Because only an acute intervention was performed in the present study, the occupancy might actually be relatively lower. Aripiprazole treatment has been shown to be well tolerated with a dose up to 30 mg/day [23], and the optimal

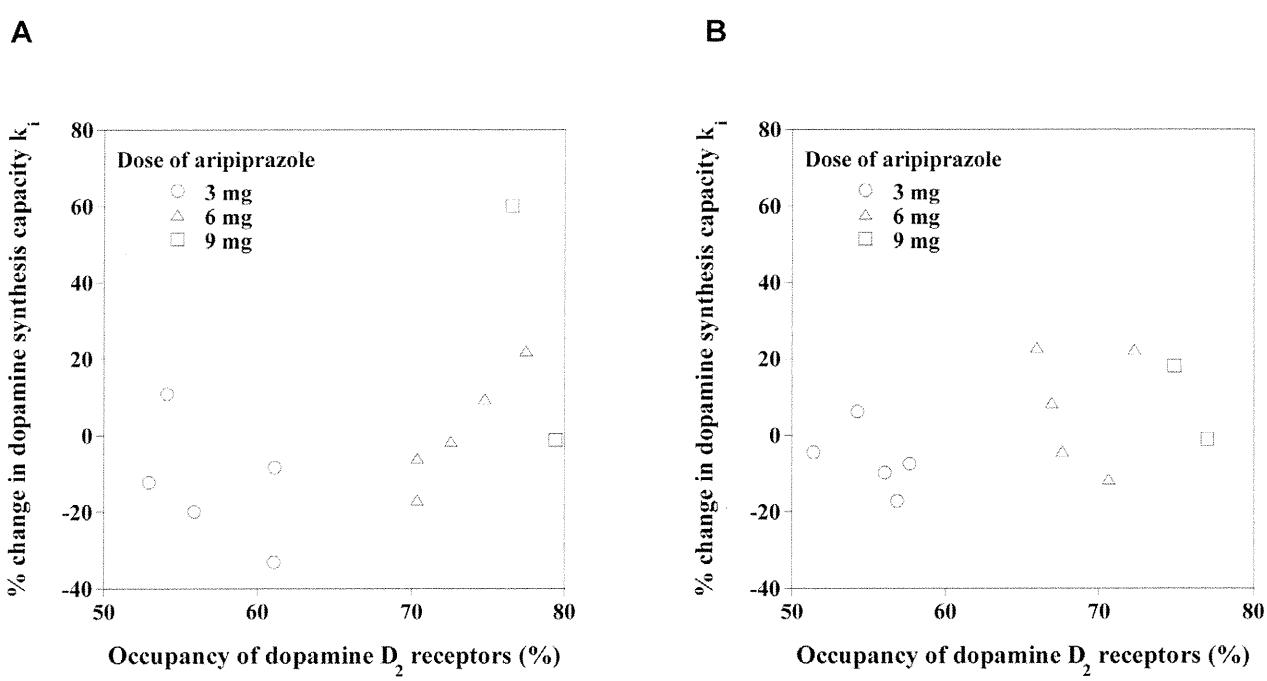

Figure 3. Relations between the occupancy of dopamine D_2 receptors and the percentage change in k_i by drug challenge with aripiprazole in the caudate (A) and putamen (B).
doi:10.1371/journal.pone.0046488.g003

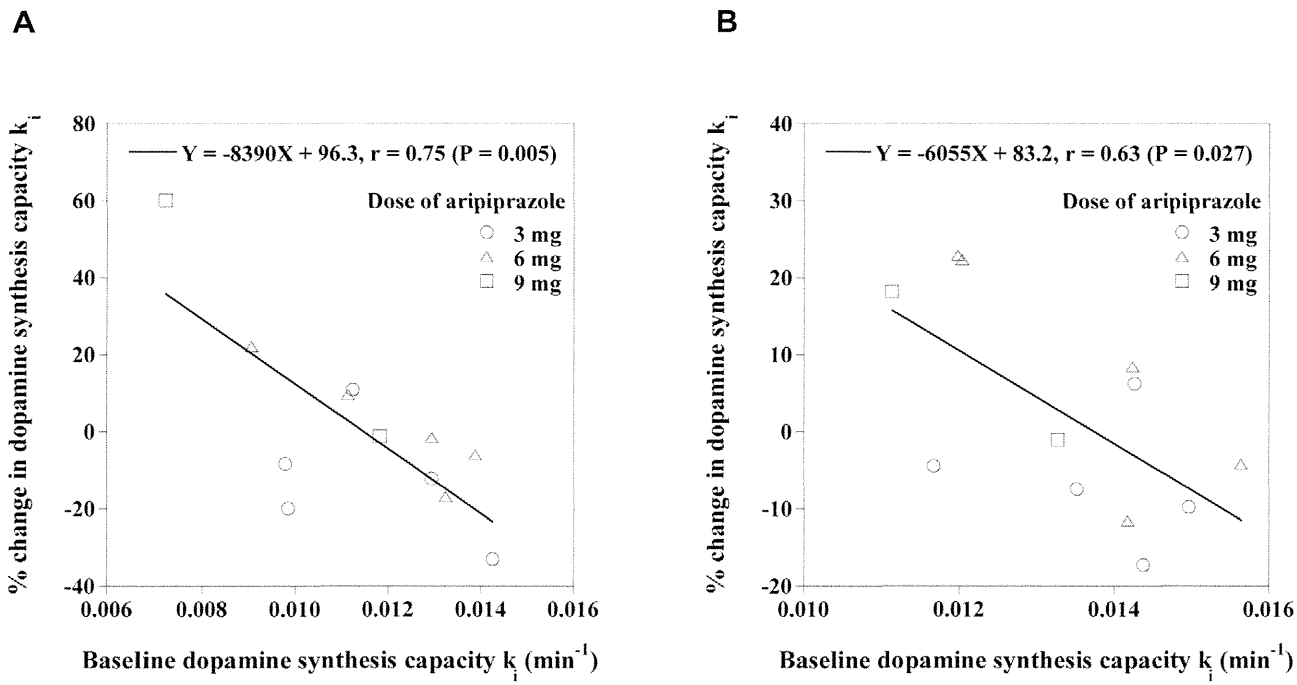

Figure 4. Relations between k_i in the baseline study and the percentage changes in k_i by drug challenge with aripiprazole in the caudate (A) and putamen (B).
doi:10.1371/journal.pone.0046488.g004

dose was reported to be 10 mg/day [4]. The doses of aripiprazole administered in this study (3–9 mg) were smaller than those doses. Since the starting dose of aripiprazole was set at 6–12 mg/day in Japan, from an ethical standpoint, a relatively small dose was used in the present study [24]. However, the chronic effects of relatively large doses of aripiprazole on dopamine synthesis capacity should be investigated in patients with schizophrenia in the future. In addition, the relation between changes in dopamine synthesis capacity and changes in clinical symptoms should also be investigated to confirm meaning of stabilizing effects of aripiprazole on dopamine synthesis capacity.

Aripiprazole also has an antagonistic action on serotonin 5-HT_{2A} receptors and a partial agonistic action on 5-HT_{1A} receptors with relatively high affinity [5]. The 5-HT_{2A} receptor antagonists have been reported to modulate endogenous dopamine release [25], and to reduce extrapyramidal side effects [26–28]. Since aripiprazole has an antagonistic action on 5-HT_{2A} receptors, it may modulate endogenous dopamine release. These reports suggest that changes in dopamine synthesis capacity by the administration of aripiprazole might be due not only to pharmacological effects on dopaminergic autoreceptors, but also on serotonin 5-HT_{2A} receptors similar to our previous report on risperidone [14]. To clarify this, additional studies using the same design and a selective antagonist for dopamine D_2 receptors, such as sulpiride, should be performed [14].

In conclusion, dopamine D_2 receptor bindings and dopamine synthesis capacities at resting condition and after oral administration of a single dose of the partial agonist antipsychotic aripiprazole were measured in the same human subjects. While dose-corresponding occupancy of dopamine D_2 receptors was observed, no significant changes in dopamine synthesis capacity by aripiprazole administration were observed. In addition, no significant correlation between occupancy of dopamine D_2 receptors and changes in dopamine synthesis capacity by aripiprazole was observed. On the other hand, a significant negative correlation was observed between baseline and aripiprazole-induced changes in dopamine synthesis capacities, indicating that the partial agonist antipsychotic aripiprazole can be considered as having a stabilizing effect on dopamine synthesis capacity, the same as antagonist antipsychotic drugs. This suggests that the therapeutic effects of aripiprazole in schizophrenia are possibly related to the stabilizing effects on dopaminergic neurotransmission responsivity.

Methods

Subjects

The study was approved by the Ethics and Radiation Safety Committees of the National Institute of Radiological Sciences, Chiba, Japan. Twelve healthy men (23–34 years of age, 24.1±3.2 years [mean ± SD]) were recruited and written informed consent was obtained. The subjects were free of somatic, neurological and psychiatric disorders according to their medical history and magnetic resonance (MR) imaging of the brain. No histories of current or previous drug abuse were revealed by interviews.

PET procedures

All PET studies were performed with a Siemens ECAT Exact HR+ system, providing 63 sections with an axial field of view of 15.5 cm [29]. Intrinsic spatial resolution was 4.3 mm in-plane and 4.2 mm full-width at half maximum (FWHM) axially. With a Hanning filter (cutoff frequency: 0.4 cycle/pixel), the reconstructed in-plane resolution was 7.5 mm FWHM. Data were acquired in three-dimensional mode. Scatter was corrected by a single scatter simulation technique [30]. A 10-min transmission scan using a ^{68}Ge-^{68}Ga line source was performed for attenuation correction. A head fixation device with thermoplastic attachments for individual fit was used to minimize head movement during the PET measurements.

PET studies were performed under resting condition (baseline study) and oral administration of aripiprazole (drug challenge study) on separate days. The interval between the 2 studies was 7 days in 7 subjects, and 14 days in 5 subjects. In each study, both PET scans with [^{11}C]raclopride and L-[β-^{11}C]DOPA were performed sequentially. Dynamic PET scanning was performed for 60 minutes following an intravenous rapid bolus injection of [^{11}C]raclopride. Then, one hour later, dynamic PET scanning was performed for 89 minutes after intravenous rapid bolus injection of L-[β-^{11}C]DOPA. The frame sequence consisted of twelve 20-sec frames, sixteen 1-min frames, and ten 4-min frames for [^{11}C]raclopride, and seven 1-min frames, five 2-min frames, four 3-min frames, and twelve 5-min frames for L-[β-^{11}C]DOPA. The radioactivity injected was 218–237 MBq and 364–392 MBq in the baseline studies, and 199–233 MBq and 364–415 MBq in the drug challenge studies for [^{11}C]raclopride and L-[β-^{11}C]DOPA, respectively. Specific radioactivity was 162–239 GBq/μmol and 24–124 GBq/μmol in the baseline studies, and 125–253 GBq/μmol and 17–273 GBq/μmol in the drug challenge studies for [^{11}C]raclopride and L-[β-^{11}C]DOPA, respectively. A venous blood sample was taken at the beginning of L-[β-^{11}C]DOPA PET scanning to measure natural neutral amino acid (NAA) concentration in plasma. The NAA concentration was measured by HPLC (L-8500 amino acid analyzer system, Hitachi Corp., Tokyo, Japan). The amino acids are phenylalanine, tryptophan, leucine, methionine, isoleucine, tyrosine, histidine, valine and threonine, which are transported via the same carrier at the blood-brain barrier as L-DOPA [31]. The weighted sum of the NAAs, which was the L-DOPA corresponding concentration of the nine NAAs for the carrier system, was calculated according to our previous work [32].

In the drug challenge studies, aripiprazole at 3–9 mg was orally administered 3.5 hours before the start of PET scanning with [^{11}C]raclopride. The aripiprazole dose was 3 mg in 5 subjects, 6 mg in 5 subjects, and 9 mg in 2 subjects. To estimate the plasma concentration of aripiprazole and its active metabolite, dehydroaripiprazole, venous blood sampling was performed at the start and end of each PET scan [33]. The plasma concentrations of aripiprazole and dehydroaripiprazole, which showed partial agonist effects similar to those of aripiprazole, were determined by the method of validated liquid chromatography coupled to mass spectrometry/mass spectrometry (LC-MS/MS) [34].

All MR imaging studies were performed with a 1.5-Tesla MR scanner (Philips Medical Systems, Best, The Netherlands). Three-dimensional volumetric acquisition of a T1-weighted gradient echo sequence produced a gapless series of thin transverse sections (TE: 9.2 msec; TR: 21 msec; flip angle: 30°; field of view: 256 mm; acquisition matrix: 256×256; slice thickness: 1 mm).

Regions of interest

All MR images were coregistered to the PET images with the statistical parametric mapping (SPM2) system [35]. Regions of interest (ROIs) were drawn manually on coregistered MR images and transferred to the PET images. ROIs were defined for the cerebellar cortex, putamen, caudate head, and occipital cortex (Fig. 2). Each ROI was drawn on three adjacent sections and data were pooled to obtain the average radioactivity concentration for the whole volume of interest. To obtain regional time-activity curves, regional radioactivity was calculated for each frame, corrected for decay, and plotted versus time. ROIs were drawn by in-house software. No software correction for head movement during PET measurements was applied to the dynamic PET images.

Calculation of occupancy of dopamine D_2 receptors

For PET studies with [^{11}C]raclopride, the binding potential (BP_{ND}) was calculated by the reference tissue model method [36,37], with which the time-activity curve in the brain region is described by that in the reference region with no specific binding, assuming that both regions have the same level of nondisplaceable radioligand binding:

$$C_i(t) = R_I \cdot C_r(t) + \left(k_2 - \frac{R_I \cdot k_2}{1 + BP_{ND}}\right) \cdot C_r(t) \otimes \exp\left(-\frac{k_2 \cdot t}{1 + BP_{ND}}\right),$$

where C_i is the radioactivity concentration in a brain region; C_r is the radioactivity concentration in the reference region; R_I is the ratio of K_1/K_1' (K_1, influx rate constant for the brain region; K_1', influx rate constant for the reference region); k_2 is the efflux rate constant for the brain region; ⊗ denotes the convolution integral. In this analysis, three parameters (BP_{ND}, R_I, and k_2) were estimated by non-linear least-squares curve fitting. The cerebellum was used as reference region. Dopamine D_2 receptor occupancy by aripiprazole was calculated as follows:

$$Occupancy(\%) = 100 \cdot \frac{BP_{ND(baseline)} - BP_{ND(drug)}}{BP_{ND(baseline)}},$$

where $BP_{ND(baseline)}$ is the BP_{ND} value in the baseline study, and $BP_{ND(drug)}$ is the BP_{ND} value in the drug challenge study.

Calculation of dopamine synthesis capacity

The uptake rate constant for L-[β-^{11}C]DOPA, indicating the dopamine synthesis capacity, was estimated by graphical analysis [38–40], which allows for calculation of the uptake rate constant k_i using time-activity data in a reference brain region with no irreversible binding. The k_i values can be estimated by simple linear least-squares fitting as follows:

$$\frac{C_i(t)}{C_i'(t)} = k_i \cdot \frac{\int_0^t C_i'(\tau)d\tau}{C_i'(t)} + F \qquad t > t*,$$

where C_i and C_i' are the total radioactivity concentrations in a brain region with and without irreversible binding, respectively, and t^* is the equilibrium time of the compartment for unchanged radiotracer in brain tissue. Plotting $C_i(t)/C_i'(t)$ versus $\int_0^t C_i'(\tau)d\tau/C_i'(t)$, after time t^*, yields a straight line with the slope k_i and intercept F. In the present study, the occipital cortex was used as reference region with no irreversible binding, because this region is known to have the lowest dopamine concentration [41] and least AADC activity [42]. The equilibrium time t^* was set to be 29 min, and data plots of 29 to 89 min were used for linear least-squares fitting [32,43]. The percentage change in k_i by oral administration of aripiprazole was calculated as follows:

$$\%\ change = 100 \cdot \frac{k_{i(drug)} - k_{i(baseline)}}{k_{i(baseline)}},$$

where $k_{i(baseline)}$ is the k_i value in the baseline study, and $k_{i(drug)}$ is the k_i value in the drug challenge study.

Acknowledgments

We thank Mr. Katsuyuki Tanimoto and Mr. Takahiro Shiraishi for their assistance in performing the PET experiments at the National Institute of Radiological Sciences. We also thank Ms. Kazuko Suzuki and Ms. Izumi Izumida of the National Institute of Radiological Sciences for their help as

clinical research coordinators. Aripiprazole and dehydroaripiprazole were kindly provided by Otsuka Pharmaceutical, Co, Ltd, Tokyo, Japan.

Author Contributions

Conceived and designed the experiments: HI. Performed the experiments: HI H. Takano RA FK KT TN MS. Analyzed the data: HI H. Takano RA H. Takahashi FK KT TN MS. Contributed reagents/materials/analysis tools: HI H. Takano RA FK KT TN MS. Wrote the paper: HI H. Takano RA H. Takahashi TS.

References

1. Farde L, Wiesel FA, Halldin C, Sedvall G (1988) Central D_2-dopamine receptor occupancy in schizophrenic patients treated with antipsychotic drugs. Archives of General Psychiatry 45: 71–76.
2. Baron JC, Martinot JL, Cambon H, Boulenger JP, Poirier MF, et al. (1989) Striatal dopamine receptor occupancy during and following withdrawal from neuroleptic treatment: correlative evaluation by positron emission tomography and plasma prolactin levels. Psychopharmacology 99: 463–472.
3. Nyberg S, Farde L, Eriksson L, Halldin C, Eriksson B (1993) 5-HT_2 and D_2 dopamine receptor occupancy in the living human brain. A PET study with risperidone. Psychopharmacology 110: 265–272.
4. Sparshatt A, Taylor D, Patel MX, Kapur S (2010) A systematic review of aripiprazole-dose, plasma concentration, receptor occupancy, and response: implications for therapeutic drug monitoring. J Clin Psychiatry 71: 1447–1456.
5. Lieberman JA (2004) Dopamine partial agonists: a new class of antipsychotic. CNS Drugs 18: 251–267.
6. Gjedde A, Reith J, Dyve S, Leger G, Guttman M, et al. (1991) Dopa decarboxylase activity of the living human brain. Proc Natl Acad Sci U S A 88: 2721–2725.
7. Cumming P, Ase A, Laliberte C, Kuwabara H, Gjedde A (1997) In vivo regulation of DOPA decarboxylase by dopamine receptors in rat brain. J Cereb Blood Flow Metab 17: 1254–1260.
8. Torstenson R, Hartvig P, Langstrom B, Bastami S, Antoni G, et al. (1998) Effect of apomorphine infusion on dopamine synthesis rate relates to dopaminergic tone. Neuropharmacology 37: 989–995.
9. Danielsen EH, Smith D, Hermansen F, Gjedde A, Cumming P (2001) Acute neuroleptic stimulates DOPA decarboxylase in porcine brain in vivo. Synapse 41: 172–175.
10. Carlsson A, Lindqvist M (1963) Effect Of Chlorpromazine Or Haloperidol On Formation Of 3methoxytyramine And Normetanephrine In Mouse Brain. Acta Pharmacol Toxicol (Copenh) 20: 140–144.
11. Der-Ghazarian T, Charntikov S, Varela FA, Crawford CA, McDougall SA (2010) Effects of repeated and acute aripiprazole or haloperidol treatment on dopamine synthesis in the dorsal striatum of young rats: comparison to adult rats. J Neural Transm 117: 573–583.
12. Vernaleken I, Kumakura Y, Cumming P, Buchholz HG, Siessmeier T, et al. (2006) Modulation of [^{18}F]fluorodopa (FDOPA) kinetics in the brain of healthy volunteers after acute haloperidol challenge. Neuroimage 30: 1332–1339.
13. Grunder G, Vernaleken I, Muller MJ, Davids E, Heydari N, et al. (2003) Subchronic haloperidol downregulates dopamine synthesis capacity in the brain of schizophrenic patients in vivo. Neuropsychopharmacology 28: 787–794.
14. Ito H, Takano H, Takahashi H, Arakawa R, Miyoshi M, et al. (2009) Effects of the antipsychotic risperidone on dopamine synthesis in human brain measured by positron emission tomography with L-[β-^{11}C]DOPA: a stabilizing effect for dopaminergic neurotransmission? J Neurosci 29: 13730–13734.
15. Yokoi F, Grunder G, Biziere K, Stephane M, Dogan AS, et al. (2002) Dopamine D_2 and D_3 receptor occupancy in normal humans treated with the antipsychotic drug aripiprazole (OPC 14597): a study using positron emission tomography and [^{11}C]raclopride. Neuropsychopharmacology 27: 248–259.
16. Mamo D, Graff A, Mizrahi R, Shammi CM, Romeyer F, et al. (2007) Differential effects of aripiprazole on D_2, 5-HT_2, and 5-HT_{1A} receptor occupancy in patients with schizophrenia: a triple tracer PET study. Am J Psychiatry 164: 1411–1417.
17. Grunder G, Fellows C, Janouschek H, Veselinovic T, Boy C, et al. (2008) Brain and plasma pharmacokinetics of aripiprazole in patients with schizophrenia: an [^{18}F]fallypride PET study. Am J Psychiatry 165: 988–995.
18. Kegeles LS, Slifstein M, Frankle WG, Xu X, Hackett E, et al. (2008) Dose-occupancy study of striatal and extrastriatal dopamine D_2 receptors by aripiprazole in schizophrenia with PET and [^{18}F]fallypride. Neuropsychopharmacology 33: 3111–3125.
19. Kikuchi T, Tottori K, Uwahodo Y, Hirose T, Miwa T, et al. (1995) 7-(4-[4-(2,3-Dichlorophenyl)-1-piperazinyl]butyloxy)-3,4-dihydro-2(1H)-quinolinon e (OPC-14597), a new putative antipsychotic drug with both presynaptic dopamine autoreceptor agonistic activity and postsynaptic D_2 receptor antagonistic activity. J Pharmacol Exp Ther 274: 329–336.
20. Vernaleken I, Kumakura Y, Buchholz HG, Siessmeier T, Hilgers RD, et al. (2008) Baseline [^{18}F]-FDOPA kinetics are predictive of haloperidol-induced changes in dopamine turnover and cognitive performance: a positron emission tomography study in healthy subjects. Neuroimage 40: 1222–1231.
21. Grace AA (1991) Phasic versus tonic dopamine release and the modulation of dopamine system responsivity: a hypothesis for the etiology of schizophrenia. Neuroscience 41: 1–24.
22. Oshibuchi H, Inada K, Sugawara H, Ishigooka J (2009) Aripiprazole and haloperidol suppress excessive dopamine release in the amygdala in response to conditioned fear stress, but show contrasting effects on basal dopamine release in methamphetamine-sensitized rats. Eur J Pharmacol 615: 83–90.
23. Potkin SG, Saha AR, Kujawa MJ, Carson WH, Ali M, et al. (2003) Aripiprazole, an antipsychotic with a novel mechanism of action, and risperidone vs placebo in patients with schizophrenia and schizoaffective disorder. Arch Gen Psychiatry 60: 681–690.
24. Takahata K, Ito H, Takano H, Arakawa R, Fujiwara H, et al. (2012) Striatal and extrastriatal dopamine D_2 receptor occupancy by the partial agonist antipsychotic drug aripiprazole in the human brain: a positron emission tomography study with [^{11}C]raclopride and [^{11}C]FLB457. Psychopharmacology (Berl), in press.
25. Pehek EA, McFarlane HG, Maguschak K, Price B, Pluto CP (2001) M100,907, a selective 5-HT_{2A} antagonist, attenuates dopamine release in the rat medial prefrontal cortex. Brain Res 888: 51–59.
26. Balsara JJ, Jadhav JH, Chandorkar AG (1979) Effect of drugs influencing central serotonergic mechanisms on haloperidol-induced catalepsy. Psychopharmacology (Berl) 62: 67–69.
27. Korsgaard S, Gerlach J, Christensson E (1985) Behavioral aspects of serotonin-dopamine interaction in the monkey. Eur J Pharmacol 118: 245–252.
28. Hicks PB (1990) The effect of serotonergic agents on haloperidol-induced catalepsy. Life Sci 47: 1609–1615.
29. Brix G, Zaers J, Adam LE, Bellemann ME, Ostertag H, et al. (1997) Performance evaluation of a whole-body PET scanner using the NEMA protocol. J Nucl Med 38: 1614–1623.
30. Watson CC, Newport D, Casey ME (1996) A single scatter simulation technique for scatter correction in 3D PET. In: Grangeat P, Amans JL, editors. Three-dimensional image reconstruction in radiology and nuclear medicine. Dordrecht, The Netherlands: Kluwer Academic Publishers. pp. 255–268.
31. Sugaya Y, Sasaki Y, Goshima Y, Kitahama K, Kusakabe T, et al. (2001) Autoradiographic studies using L-[^{14}C]DOPA and L-DOPA reveal regional Na^+-dependent uptake of the neurotransmitter candidate L-DOPA in the CNS. Neuroscience 104: 1–14.
32. Ito H, Ota M, Ikoma Y, Seki C, Yasuno F, et al. (2006) Quantitative analysis of dopamine synthesis in human brain using positron emission tomography with L-[β-^{11}C]DOPA. Nucl Med Commun 27: 723–731.
33. Molden E, Lunde H, Lunder N, Refsum H (2006) Pharmacokinetic variability of aripiprazole and the active metabolite dehydroaripiprazole in psychiatric patients. Ther Drug Monit 28: 744–749.
34. Wood MD, Scott C, Clarke K, Westaway J, Davies CH, et al. (2006) Aripiprazole and its human metabolite are partial agonists at the human dopamine D_2 receptor, but the rodent metabolite displays antagonist properties. Eur J Pharmacol 546: 88–94.
35. Friston KJ, Frith CD, Liddle PF, Dolan RJ, Lammertsma AA, et al. (1990) The relationship between global and local changes in PET scans [see comments]. J Cereb Blood Flow Metab 10: 458–466.
36. Lammertsma AA, Bench CJ, Hume SP, Osman S, Gunn K, et al. (1996) Comparison of methods for analysis of clinical [^{11}C]raclopride studies. Journal of Cerebral Blood Flow & Metabolism 16: 42–52.
37. Lammertsma AA, Hume SP (1996) Simplified reference tissue model for PET receptor studies. Neuroimage 4: 153–158.
38. Patlak CS, Blasberg RG (1985) Graphical evaluation of blood-to-brain transfer constants from multiple-time uptake data. Generalizations. J Cereb Blood Flow Metab 5: 584–590.
39. Gjedde A (1988) Exchange diffusion of large neutral amino acids between blood and brain. In: Rakic L, Begley DJ, Davson H, Zlokovic BV, editors. Peptide and amino acid transport mechanisms in the cerebral nervous system. New York: Stockton Press. pp. 209–217.
40. Hartvig P, Agren H, Reibring L, Tedroff J, Bjurling P, et al. (1991) Brain kinetics of L-[β-^{11}C]dopa in humans studied by positron emission tomography. J Neural Transm Gen Sect 86: 25–41.
41. Brown RM, Crane AM, Goldman PS (1979) Regional distribution of monoamines in the cerebral cortex and subcortical structures of the rhesus monkey: concentrations and in vivo synthesis rates. Brain Res 168: 133–150.
42. Lloyd KG, Hornykiewicz O (1972) Occurrence and distribution of aromatic L-amino acid (L-DOPA) decarboxylase in the human brain. J Neurochem 19: 1549–1559.
43. Ito H, Shidahara M, Takano H, Takahashi H, Nozaki S, et al. (2007) Mapping of central dopamine synthesis in man using positron emission tomography with L-[β-^{11}C]DOPA. Ann Nucl Med 21: 355–360.

PLOS ONE

Association between Striatal Subregions and Extrastriatal Regions in Dopamine D_1 Receptor Expression: A Positron Emission Tomography Study

Hironobu Fujiwara[1], Hiroshi Ito[2]*, Fumitoshi Kodaka[1], Yasuyuki Kimura[1], Harumasa Takano[1], Tetsuya Suhara[1]

1 Clinical Neuroimaging Team, Molecular Neuroimaging Program, Molecular Imaging Center, National Institute of Radiological Sciences, Chiba, Japan, **2** Biophysics Program, Molecular Imaging Center, National Institute of Radiological Sciences, Chiba, Japan

Abstract

The mesencephalic dopamine (DA) system is the main DA system related to affective and cognitive functions. The system consists of two different cell groups, A9 and A10, which originate from different regions of the midbrain. The striatum is the main input from the midbrain, and is functionally organized into associative, sensorimotor and limbic subdivisions. At present, there have been few studies investigating the associations of DA functions between striatal subdivisions and extrastriatal regions. The aim of this study was to investigate the relationship of DA D_1 receptor (D_1R) expression between striatal subdivisions and extrastriatal regions in humans using positron emission tomography (PET) with voxel-by-voxel whole brain analysis. The PET study was performed on 30 healthy subjects using [^{11}C]SCH23390 to measure D_1R expression. Parametric images of binding potentials (BP_{ND}) were created using the simplified reference tissue model. Regions of interest were defined for striatal subdivisions. Multiple regression analysis was undertaken to determine extrastriatal regions that were associated with each striatal subdivision in BP_{ND} using statistical parametric mapping 5. The BP_{ND} values of associative, sensorimotor and limbic subdivisions were similarly correlated with those of multiple brain regions. Regarding the interrelationships among striatal subdivisions, mutual correlations were found among associative, sensorimotor and limbic subdivisions in BP_{ND} as well. The relationships in BP_{ND} between striatal subdivisions and extra-striatal regions suggest that differential striatal subdivisions and extrastriatal regions have a similar biological basis of D_1R expression. Different DA projections from the midbrain did not explain the associations between striatal subdivisions and extrastriatal regions in D_1R expression, and the DA-related neural networks among the midbrain, striatum and the other regions would contribute to a similar D_1R expression pattern throughout the whole brain.

Citation: Fujiwara H, Ito H, Kodaka F, Kimura Y, Takano H, et al. (2012) Association between Striatal Subregions and Extrastriatal Regions in Dopamine D_1 Receptor Expression: A Positron Emission Tomography Study. PLoS ONE 7(11): e49775. doi:10.1371/journal.pone.0049775

Editor: Bernard Le Foll, Centre for Addiction and Mental Health, Canada

Received July 17, 2012; **Accepted** October 11, 2012; **Published** November 21, 2012

Funding: This study was supported by a consignment expemse for Molecular Imaging Program on "Research Base for PET Diagnosis" from the Ministry of Education, Culture, Sports, Science and Technology (MEXT), Japanese Government. The funders had no role in study design, data collection and analysis, decision to publish, or preparation of the manuscript.

Competing Interests: The authors have declared that no competing interests exist.

* E-mail: hito@nirs.go.jp

Introduction

The mesencephalic dopamine (DA) system is the main DA system, and it is related to affective and cognitive functions such as reward processing. The system is roughly divided into different groups, A9 and A10, whose cells are located in different regions of the midbrain, the substantia nigra (SN) and the ventral tegmental area (VTA), respectively. These different projections have been reported in rats, monkeys and humans [1,2,3]. The striatum provides the main input from the midbrain. Histologically, this region is not uniform, and it is functionally divided into striatal subdivisions termed associative (AST), sensorimotor (SMST) and limbic (LST), which process information related to cognitive, sensorimotor, and emotional functions, respectively [4]. The concept is based on neural networks termed "Cortico-striatal-thalamo-cortical loops" [5]. In brief, functionally different networks between each striatal subdivision and extrastriatal regions would exist through dopaminergic, glutaminergic and gamma-butylic amino acid (GABA) neurotransmissions, and these neurotransmissions interact with each other [6]. Regarding DA projections, A9 would project to the dorsal striatum (AST and SMST) and A10 to LST. A10 would have direct projections to cortical regions as well.

Ample literature describes the differential DA pathways and the distribution of DA receptors by *in vitro* methods, including distinct DA projections from the midbrain to the dorsal and ventral striatum [7], region-by-region differences of DA receptor distribution in the cortex [8], and alterations of DA projections in several neuropsychiatric illnesses [9,10]. Regarding neuroimaging studies, several reports have suggested the relationships between DA functions and cognitive functions [11,12], and the association of DA functions with the pathophysiology of neuropsychiatric illnesses [10,13]. Thus, it is worthwhile investigating DA functions in their relationships among different regions of the human brain by *in vivo* methods, especially between the DA receptor-rich regions (striatum) and other regions, which could provide new insights for studies of DA-

related cognitive functions and pathophysiologies of neuropsychiatric disorders.

However, at present, there have been few neuroimaging studies that directly demonstrated the relationship between striatal subdivisions and extrastriatal (ie., cortical) regions, which also have DA projections from the midbrain in DA receptor expressions. Clarification of this issue would lead to a better understanding of DA functions in region-by-region relationships, considering the manner of DA projections from the midbrain and the distinction of their targets, that is, the most DA-rich region, the striatum and cortical regions. In this sense, one possibility might be that DA receptor expressions are regulated differentially according to their origin of DA projection.

However, very recently, one positron emission tomography (PET) study has suggested that there was no relationship between cortical DA D_2 receptor (D_2R) densities and those of striatal regions [14]. Regarding another dopamine receptor subtype, DA D_1 receptor (D_1R), Rieckmann et al. reported that subdivisional striatal D_1R densities are similarly associated with those of multiple cortical regions, concluding that D_1R expressions in striatal and extrastriatal regions are not regulated independently, despite DA projections from different midbrain areas. In their study [15], interregional association of D_1R was assessed by a conventional method in terms of the analysis of PET images, that is, regions of interests (ROIs) were traced manually on each individual subject's image without spatial normalization. This method is potentially advantageous in preserving the information of raw images, but the results may partially depend on the rater's procedure. Thus, the conventional manual tracing method and another method, voxel-by-voxel analysis, could be expected to complement each other in respect to confirming their reliability and validity.

The aim of the present study was to investigate the relationship between striatal subdivisions and extrastriatal regions in DA D_1 receptor (D_1R) expression using PET in healthy humans by voxel-by-voxel analysis, a potentially more objective method than the manual ROI-tracing method used by Rieckmann et al. [15]. We hypothesized that D_1R availability of the striatum would be associated with the availability of extrastriatal regions regardless of its differential subdivisions, i.e., the D_1R expressions of AST, SMST and LST would be similarly correlated with the expressions of extrastriatal regions.

Methods

Ethics Statement

In accordance with the Helsinki Declaration of Human Rights (2000), written informed consent was obtained from all volunteers after detailed explanation of the study. This study protocol was approved by the Ethics and Radiation Safety Committees of the National Institute of Radiological Sciences, Chiba, Japan.

Subjects

A total of 30 healthy men (age = 25.4±5.9 [mean ± SD]) were recruited, and they gave their written informed consent for participation in this study. The subjects were free of somatic, neurological or psychiatric disorders on the basis of their medical history and magnetic resonance imaging (MRI) of the brain. They had no history of current or previous drug abuse.

PET Procedures

The PET system ECAT EXACT HR+(CTI-Siemens, Knoxville, TN) was used for all PET studies. The system provides 63 planes with a 15.5 cm axial field of view. The intrinsic spatial resolution was 4.3 mm in-plane and 4.2 mm full-width at half maximum (FWHM) axially. With a Hanning filter (cut-off frequency: 0.4 cycle/pixel), the reconstruct in-plane resolution was 7.5 mm FWHM. Data were acquired in three-dimensional mode. Scatter was corrected [16]. A head fixation device with thermoplastic attachments for individual fit minimized head movement during PET measurements. A 10-min transmission scan using a ^{68}Ge-^{68}Ga line source was performed for correction of attenuation. After intravenous rapid bolus injection of [^{11}C]SCH23390, data were acquired for 60 min in a consecutive series of time frames. The frame sequences consisted of thirty 2-min frames. Injected radioactivity was 197–235 MBq and specific radioactivity was 23–81 GBq/μmol at the time of injection.

MRI Procedures

All MRI scanning was performed with a 1.5-T MR scanner (Philips Medical Systems, Best, The Netherlands). Three-dimensional volumetric acquisition of a T1-weighted gradient echo sequence produced a gapless series of thin transverse sections (TE: 9.2 ms; TR: 21 ms; flip angle: 30°; field of view: 256 mm; acquisition matrix: 256×256; slice thickness: 1 mm).

Calculation of Parametric Images

We used PMOD 3.1 software (PMOD Technologies Ltd., Zurich, Switzerland) for all the steps of the image processing and analysis. All MR images were coregistered to the PET images. MR images were transformed into standard brain size and shape by linear and non-linear parameters (anatomic standardization). The brain templates for anatomic standardization were Montreal Neurological Institute (MNI)/International Consortium for Brain Mapping (ICBM) 152 T1 templates as supplied with the PMOD software. All PET images were also transformed into standard brain size and shape by using the same parameters as for the MR images. Thus, brain images of all 30 subjects had the same anatomic format.

Binding potentials (BP_{ND}) were calculated by the reference tissue model method on a voxel-by-voxel basis [17,18]. BP_{ND} refers to the ratio of specifically bound radioligand to that of nondisplaceable radioligand in tissue at equilibrium. BP_{ND} is the typical measurement from reference tissue methods, as it compares the concentration of radioligand in receptor-rich to receptor-free regions [19]. In this study, parametric images, in which each voxel has its own BP_{ND} value, were generated using the cerebellum, a receptor-free region, as reference tissue.

Data Analysis

ROIs were drawn on a standardized and averaged MR image of all the subjects, and this ROI object map was applied to the parametric images of each of the 30 subjects, that is, only one ROI object map was applied to the parametric images of each of the 30 subjects completely in the same manner. Thus, this method is a more objective way to measure BP_{ND} values than that with different ROIs for each subject. Boundaries for ROIs of striatal functional subdivisions were defined for each striatal subregion [20,21]. The definition of the "functional subdivisions" was as follows: AST consisted of the precommissural dorsal caudate, precommissural dorsal putamen, and postcommissural caudate, and the BP_{ND} values of AST were calculated as the spatially weighted average of these three subregions; SMST and LST corresponded to the postcommissural putamen and ventral striatum, respectively (Figure 1).

Regarding the statistics, multiple regression analysis was performed by statistical parametric mapping (SPM5, Wellcome Trust Centre for Neuroimaging, London, UK) on a voxel-by-voxel

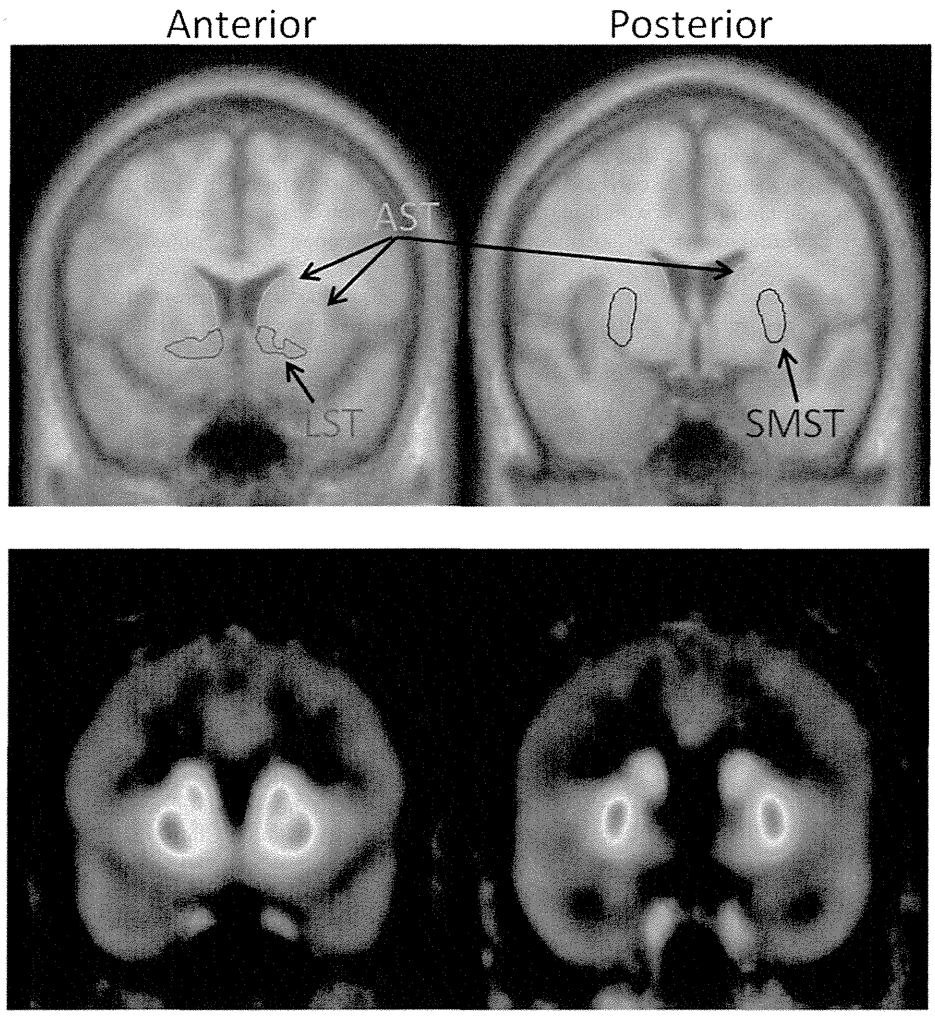

Figure 1. Definition of striatal functional subdivisions. Upper panel: MR images and regions of interest. Lower panel: parametric images corresponding to MR images in the upper panel.
doi:10.1371/journal.pone.0049775.g001

basis after the BP_{ND} values of the striatal subdivisions were obtained. The values of each striatal subdivision were used as covariates of interest in the design matrix to determine the regions correlating with each striatal subdivision in terms of their D_1R expression. Statistical thresholds were as follows: false recovery rate (FDR) $p<0.05$, extent threshold = 100 voxels. The results of the correlation were visualized in statistical parametric maps.

To confirm the result of voxel-by-voxel analysis with SPM5, Pearson's correlation coefficient was also calculated using the actual BP_{ND} values in extrastriatal regions with SPSS version 18.0. The ROIs of extrastriatal regions included thalamic, cingulate, prefrontal, temporal and occipital regions, and the boundaries for the ROIs were based on previous reports [21,22].

Results

The BP_{ND} values of AST, SMST, and LST were 1.61 ± 0.26, 1.70 ± 0.24, and 1.36 ± 0.19, respectively. The values were quite similar to our previous data for measuring D_1R in the striatum [22].

By voxel-by-voxel analysis, the values of each striatal subdivision (i.e., AST, SMST and LST) were positively correlated with those of multiple brain regions, i.e., frontal, temporal, parietal and occipital regions in a similar manner (Figure 2). Regarding the interrelationships among striatal subdivisions, mutual positive correlation was found among AST, SMST and LST in D_1R BP_{ND} (Figure 2).

In addition, the interregional positive correlations in BP_{ND} were revealed to be significant by the ROI analysis, that is, by the analysis using SPSS software with the actual BP_{ND} values of each ROI (Figure 3).

Discussion

The critical role of the DA system in cognitive functions has been suggested repeatedly, and abnormalities of the system have also been implicated in the pathophysiology of several neuropsychiatric disorders such as schizophrenia [13,23] and Parkinson's disease [10]. The main focus of those findings was restricted exclusively to D_1R functions or abnormalities in terms of their expression levels, distribution, and localization in several brain regions. In this sense, there is little evidence that refers to a direct association of a DA-rich region (the striatum) and extrastriatal regions, where DA receptors are present. It has been suggested that cognitive functions such as executive function would be associated with the manner of interregional relationship in D_1R

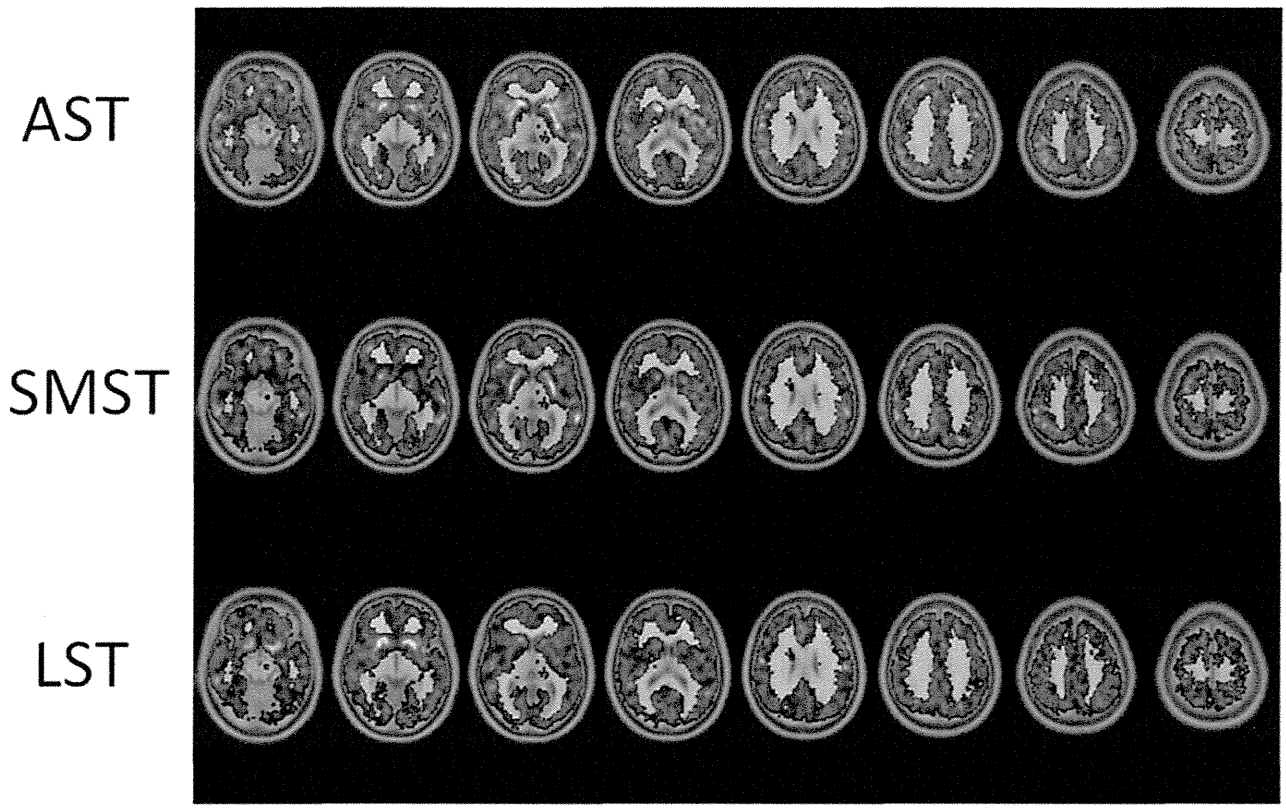

Figure 2. Correlation map of striatal functional subdivisions and extrastriatal regions, in addition to that of within striatal subdivisions. Correlations in brighter color (yellow) represent higher ones in terms of magnitude than those in red.
doi:10.1371/journal.pone.0049775.g002

expression [15], and therefore it would be worthwhile investigating the interregional patterns of bindings for studies of neuropsychiatric disorders in which cognitive dysfunction based on DA system dysregulation is considered to exist, such as schizophrenia and Parkinson's disease.

We could replicate the findings of a previous study by Rieckmann et al. [15] that demonstrated the association of striatal subdivisions and cortices by a conventional manual tracing method. The major findings of the present study were as follows: (a) BP_{ND} values of all striatal subdivisions (i.e., AST, SMST and LST) were significantly correlated with those of multiple brain regions on a voxel-by-voxel basis: (b) regarding the interrelationships among striatal subdivisions, they were also mutually correlated in their BP_{ND} values.

These results suggest that D_1R expressions in striatal subdivisions and extrastriatal regions are regulated uniformly. This could be explained by the complex connections of DA pathways throughout the whole brain. DA innervations from VTA and SN differentially project to striatal subdivisions as well as the cortical regions through A9 and A10, whereas glutaminergic innervations from cortical regions project to both VTA and SN via the striatum. Regarding the connection of the midbrain with the striatum, the midbrain has reciprocal projections both to (DA) and from (GABA) the striatum, with overlapping. Thus, DA pathways are connected via these pathways [4,24], and this would lead to similarity of the regulation of D_1R expressions among multiple brain areas, although differential DA projection from the midbrain (i.e., A9 and A10) is a part of the DA-related neural network.

Furthermore, striatal outputs to the cortex, which are altered by D_1R stimulation/blockade, would affect immediate-early gene expressions such as c-fos expression (as functional markers) in cortical regions [25]. If the D_1R function in each striatal

	AST	SMST	LST	ACC	MPFC	DLPFC	OFC	Temporal	Occipital	Parietal	Thalamus
AST		643**	587**	436**	361**	247**	507**	637**	188	305**	372**
SMST			363**	583**	333**	233**	622**	706**	086	338**	410**
LST				215**	185*	136*	327**	348**	079	162*	228**

Figure 3. Correlations between striatum and extrastriatal regions and intercorrelations among striatal subdivisions in dopamine D_1 receptor BP_{ND}. **P<0.01, *P<0.05. Correlations in red: intercorrelations among striatal subdivisions. Correlations in blue: correlations between striatal subdivisions and extrastriatal regions. R^2 values are presented for the correlations.
doi:10.1371/journal.pone.0049775.g003

subdivision uniformly affects the expressions in cortical regions, each striatal subdivision and the cortical regions are mutually correlated in a similar manner. In this study, interrelationships among striatal subdivisions were found in their BP_{ND} values, thus providing a convincing explanation for the uniform relationships between different striatal subdivisions and cortical regions in their D_1R expression.

Finally, D_1R expressions throughout the whole brain might be generally (genetically) associated with each other, i.e., the larger the expressions in the striatum, the larger in the other regions as well. However, further investigations including postmortem and animal studies would be needed to clarify the genetic influence on the D_1R expression throughout the whole brain.

Several limitations need to be pointed out in the current study. First, the age of the participants was restricted to a relatively younger generation. Second, the subjects were all males. Further study with both male and female participants of a wider age range will be needed to give the findings a more generalized significance. Third, the reference tissue model has a potential limitation in terms of its theory, the assumption of the same non-specific binding throughout the whole brain, which might lead to a systemic bias in respect to between-region correlations of the bindings. To our knowledge, there has been no study that suggested a higher variation of receptor density corresponding to BP_{ND} in different regions compared with that of non-specific binding in the human population. However, the non-specific binding in tissue has been reported to be generally constant across species including humans [26]. Thus, the correlation of the current study would reflect the relationship in receptor density in itself rather than inter-individual variations of non-specific binding. Further theoretical and methodological improvements would be needed to assess interregional correlations of binding potentials more accurately, considering the influence of inter-individual variations in non-specific binding. Fourth, it could be argued that the interregional associations in the bindings in the current study may reflect the association in the serotonergic system in addition to the DA system because of the affinity of SCH23390 to $5\text{-}HT_{2A}$ receptors in cortical regions. However, this confounding effect of cortical $5\text{-}HT_{2A}$ binding would not be so critical in terms of the analysis of striatal and extrastriatal correlations because striatal binding reflects D_1R density only, whereas the bindings of cortical regions are significantly confounded by $5\text{-}HT_{2A}$ receptors [15]. In the present study, the BP_{ND} values of striatal and extrastriatal regions were highly correlated, and thus the correlations are not always considered to represent different receptor associations. Finally, in general, completely accurate image processing (namely, coregistration and normalization) is difficult in voxel-based analyses. In this study, the accuracy of image processing and ROI adjustment on parametric images was confirmed by visual inspection for each subject. However, at present, there is no absolute procedure in this regard because of the variation of the individual's brain in respect to its shape, size and sulcal anomaly. Further improvements in image processing technique would be necessary to raise the reliability of voxel-wise analysis.

Conclusions

In conclusion, differential striatal functional subdivisions could be associated with cortical regions in terms of D_1R expression in a similar manner. Although DA cell projections from VTA and SN innervate the striatum and extrastriatal regions via different DA pathways, DA-related neural networks throughout the whole brain including both striato-midbrain and cortical-striato connections would contribute to the association of the striatal subdivisions and extrastriatal regions in D_1R expression. Further study will be needed to clarify the mechanisms of D_1R expression regarding the interactions between DA and the other neurotransmitter systems such as glutamate, serotonin and GABA, and the mechanisms at molecular and genetic levels in the respective brain regions.

Author Contributions

Conceived and designed the experiments: HI TS HF. Performed the experiments: HI HT. Analyzed the data: HF YK FK. Wrote the paper: HF.

References

1. Dahlström A, Fuxe K (1964) A method for the demonstration of monoamine-containing nerve fibres in the central nervous system. Acta Physiol Scand 60: 293–4.
2. Di Carlo FJ, Melgar MD, Haynes LJ, Crew MC (1973) Metabolic profile of a new immunosuppressive agent, oxisuran: binding, RE stimulation, drug interaction. J Reticuloendothel Soc 14(4): 387–97.
3. Felten DL, Sladek JR Jr. (1983) Monoamine distribution in primate brain V. Monoaminergic nuclei: anatomy, pathways and local organization. Brain Res Bull 10: 171–284.
4. Joel D, Weiner I (2000) The connections of the dopaminergic system with the striatum in rats and primates: an analysis with respect to the functional and compartmental organization of the striatum. Neuroscience 96: 451–74.
5. Alexander GE, Crutcher MD (1990) Functional architecture of basal ganglia circuits: neural substrates of parallel processing. Trends Neurosci 13: 266–71.
6. Carlsson A,Waters N, Carlsson ML (1999) Neurotransmitter interactions in schizophrenia-therapeutic implications. Eur Arch Psychiatry Clin Neurosci 249: 37–43.
7. Haber SN, McFarland NR (1999) The concept of the ventral striatum in nonhuman primates. Ann N Y Acad Sci 877: 33–48.
8. Hurd YL, Suzuki M, Sedvall GC (2001) D1 and D2 dopamine receptor mRNA expression in whole hemisphere sections of the human brain. J Chem Neuroanat 22: 127–37.
9. Grace AA (1991) Phasic versus tonic dopamine release and the modulation of dopamine system responsivity: a hypothesis for the etiology of schizophrenia. Neuroscience 41: 1–24.
10. Gaspar P, Duyckaerts C, Alvarez C, Javoy-Agid F, Berger B (1991) Alterations of dopaminergic and noradrenergic innervations in motor cortex in Parkinson's disease. Ann Neurol 30: 365–74.
11. Takahashi H, Kato M, Takano H, Arakawa R, Okumura M, et al. (2008) Differential contributions of prefrontal and hippocampal dopamine D1 and D2 receptors in human cognitive functions. J Neurosci 28: 12032–12038.
12. Takahashi H, Matsui H, Camerer C, Takano H, Kodaka F, et al. (2010) Dopamine D_1 receptors and nonlinear probability weighting in risky choice,J Neurosci 30: 16567–72.
13. Suhara T, Okubo Y, Yasuno F, Sudo Y, Inoue M, et al. (2002) Decreased dopamine D2 receptor binding in the anterior cingulate cortex in schizophrenia. Arch Gen Psychiatry 59: 25–30.
14. Cervenka S, Varron A, Fransen E, Halldin C, Farde L (2010) PET studies of D2-receptor binding in striatal and extrastriatal brain regions: biochemical support in vivo for separate dopaminergic systems in humans. Synapse 64: 478–85.
15. Rieckmann A, Karlsson S, Larlsson P, Brehmer Y, Fischer H, et al. (2011) Dopamine D1 receptor associations within and between dopaminergic pathways in younger and elderly adults: link to cognitive performance. Cereb Cortex 21: 2023–32.
16. Watson CC, Newport D, Casey ME (1996) A single scatter simulation technique for scatter correction in 3D PET. In: Grangeat P, Amans JL (Eds.), Three-Dimensional Image Reconstruction in Radiology and Nuclear Medicine. Kluwer Academic Publishers, Dordrecht, The Netherlands, 255–268.
17. Gunn RN, Lammertsma AA, Hume SP, Cunningham VJ (1997) Parametric imaging of ligand-receptor binding in PET using a simplified reference region model. NeuroImage 6: 279–87.
18. Lammertsma AA, Hume SP, 1996. Simplified reference tissue model for PET receptor studies. NeuroImage 4, 153–158.
19. Innis RB, Cunningham VJ, Delforge J, Fujita M, Gjedde A, et al. (2007) Consensus nomenclature for in vivo imaging of reversibly binding radioligands. J Cereb Blood Flow Metab 27: 1533–9.
20. Martinez D, Slifstein M, Broft A, Mawlawi O, Hwang DR, et al. (2003) Imaging Human mesolimbic dopamine transmission with positron emission tomography. part II: amphetamine-induced dopamine release in the functional subdivisions of the striatum. J Cereb Blood Flow Metab 23: 285–300.

21. Abi-Dargham A, Mawlawi O, Lombard L, Gil R, Martinez D et al. (2002) Prefrontal Dopamine D1 Receptors and Working Memory in Schizophrenia. J Neurosci 22: 3708–19.
22. Ito H, Takahashi H, Arakawa R, Takano H, Suhata T (2008) Normal database of dopaminergic neurotransmission system in human brain measured by postron emission tomography. NeuroImage 39: 555–565.
23. Okubo Y, Suhara T, Suzuki K, Kobayashi K, Inoue O, et al. (1997) Decreased prefrontal dopamine D1 receptors in schizophrenia revealed by PET. Nature 385(6617): 634–6.
24. Haber SN, Fudge JL, McFarland NR (2000) Striatonigrostriatal pathways in primates form an ascending spiral from the shell to the dorsolateral striatum. J Neurosci 20: 2369–82.
25. Steiner H, Kitai ST (2000) Regulation of rat cortex function by D1 dopamine receptors in the striatum. J Neurosci 20: 5449–60.
26. Summerfield SG, Lucas AJ, Porter RA, Jeffrey P, Gunn RN, et al. (2008) Toward an improved prediction of human in vivo brain penetration. Xenobiotica 38: 1518–35.

frontiers in PSYCHOLOGY

ORIGINAL RESEARCH ARTICLE
published: 19 March 2013
doi: 10.3389/fpsyg.2013.00105

Cross-cultural differences in the processing of non-verbal affective vocalizations by Japanese and Canadian listeners

Michihiko Koeda[1,2]*, Pascal Belin[2], Tomoko Hama[3], Tadashi Masuda[4], Masato Matsuura[3] and Yoshiro Okubo[1]

[1] *Department of Neuropsychiatry, Nippon Medical School, Tokyo, Japan*
[2] *Voice Neurocognition Laboratory, Institute of Neuroscience and Psychology, College of Medical, Veterinary and Life Sciences, University of Glasgow, Glasgow, UK*
[3] *Department of Biofunctional Informatics, Tokyo Medical and Dental University, Tokyo, Japan*
[4] *Division of Human Support System, Faculty of Symbiotic Systems Science, Fukushima University, Fukushima, Japan*

Edited by:
Anjali Bhatara, Université Paris Descartes, France

Reviewed by:
Jan Van Den Stock, Katholieke Universiteit Leuven, Belgium
Keiko Ishii, Kobe University, Japan

***Correspondence:**
Michihiko Koeda, Department of Neuropsychiatry, Nippon Medical School, 1-1-5, Sendagi, Bunkyo-ku, Tokyo 113-8603, Japan.
e-mail: mkoeda@nms.ac.jp

The Montreal Affective Voices (MAVs) consist of a database of non-verbal affect bursts portrayed by Canadian actors, and high recognitions accuracies were observed in Canadian listeners. Whether listeners from other cultures would be as accurate is unclear. We tested for cross-cultural differences in perception of the MAVs: Japanese listeners were asked to rate the MAVs on several affective dimensions and ratings were compared to those obtained by Canadian listeners. Significant Group × Emotion interactions were observed for ratings of Intensity, Valence, and Arousal. Whereas Intensity and Valence ratings did not differ across cultural groups for sad and happy vocalizations, they were significantly less intense and less negative in Japanese listeners for angry, disgusted, and fearful vocalizations. Similarly, pleased vocalizations were rated as less intense and less positive by Japanese listeners. These results demonstrate important cross-cultural differences in affective perception not just of non-verbal vocalizations expressing positive affect (Sauter et al., 2010), but also of vocalizations expressing basic negative emotions.

Keywords: montreal affective voices, emotion, voice, cross-cultural differences, social cognition

INTRODUCTION

Vocal affective processing has an important role in ensuring smooth communication during human social interaction as well as facial affective processing. Facial expressions are generally recognized as the universal language of emotion (Ekman and Friesen, 1971; Ekman et al., 1987; Ekman, 1994; Izard, 1994; Jack et al., 2012): however, several studies have demonstrated cross-cultural differences in facial expression between Western and Eastern groups (Ekman and Friesen, 1971; Ekman et al., 1987; Matsumoto and Ekman, 1989; Izard, 1994; Yrizarry et al., 1998; Elfenbein and Ambady, 2002; Jack et al., 2009, 2012). Whether such cross-cultural differences also exist in the recognition of emotional vocalizations is not clear.

Most previous cross-cultural studies of auditory perception have investigated the processing of emotional Valence using word stimuli (Scherer and Wallbott, 1994; Kitayama and Ishii, 2002; Ishii et al., 2003; Min and Schirmer, 2011). One important study demonstrated cross-cultural differences in the rating of Intensity when subjects recognized meaning of the words with major emotions such as joy, fear, anger, sadness, and disgust (Scherer and Wallbott, 1994). Another previous study examined cross-cultural differences in the perception of emotional words (Kitayama and Ishii, 2002). This study indicated that native English speakers spontaneously pay more attention to verbal content than to vocal tone when they recognize emotional words, whereas native Japanese speakers spontaneously attend more to vocal tone than to verbal content. The other study has shown that Japanese are more sensitive to vocal tone compared to Dutch participants in the experiment of the multisensory perception of emotion (Tanaka et al., 2010). Further, one other study demonstrated cross-cultural differences in semantic processing of emotional words (Min and Schirmer, 2011), but found no difference in the processing of emotional prosody between native and non-native listeners. These studies suggest cross-cultural differences in auditory recognition of emotional words.

Studies of affective perception in speech prosody are made complex, in particular, by the potential interactions between the affective and the linguistic contents of speech (Scherer et al., 1984; Murray and Arnott, 1993; Banse and Scherer, 1996; Juslin and Laukka, 2003). To avoid this interaction, some studies have controlled the processing of semantic content using pseudo-words (Murray and Arnott, 1993; Schirmer et al., 2005) or pseudo-sentences (Ekman and Friesen, 1971; Pannekamp et al., 2005; Schirmer et al., 2005). The other previous study has employed a set of low-pass filtered vocal stimuli to select the final set of emotional utterances (Ishii et al., 2003), i.e., non-verbal vocalizations often accompanying strong emotional states such as laughs or screams of fear. Non-verbal affective vocalizations are ideally suited to investigations of cross-cultural differences in the perception of affective information in the voice since they eliminate the need to account for language differences between groups.

A recent study compared the perception of such non-verbal affective vocalizations by listeners from two highly different cultures: Westerners vs. inhabitants of remote Namibian villages. Non-verbal vocalizations expressing negative emotions could be recognized by the other culture much better than those expressing

positive emotions, which lead the authors to propose that a number of primarily negative emotions have vocalizations that can be recognized across cultures while most positive emotions are communicated with culture-specific signals (Sauter et al., 2010). However this difference could be specific to English vs. Namibian groups, reflecting for instance different amounts of exposure to vocalizations through media or social interactions, and might not generalize to other cultures.

In the present experiment we tested for cross-cultural differences in perception of affective vocalizations between two cultures much more comparable in socio-economic status and exposure to vocalizations: Canadian vs. Japanese participants. Stimuli consisted of the Montreal Affective Voices (MAVs; Belin et al., 2008), a set of 90 non-verbal affect bursts produced by 10 actors and corresponding to emotions of Anger, Disgust, Fear, Pain, Sadness, Surprise, Happiness, and Pleasure. The MAVs have been validated in a sample of Canadian listeners and showed high inter-reliability in judgments of emotional Intensity, Valence, and Arousal as well as hit rates in emotional recognition (Belin et al., 2008). Here, we collected affective ratings using similar procedures in Japanese listeners and compared those ratings to those obtained in the Canadian listeners. Before the experiment, we predicted that ratings of negative emotion are culturally universal although cross-cultural differences would exist in ratings of positive emotion.

MATERIALS AND METHODS

SUBJECTS

Thirty Japanese subjects (male 15, female 15) participated in this study. The average age was 22.3 ± 1.4 years. The educational years of Japanese subjects were 14.1 ± 0.3. The data of Japanese subjects were compared with 29 Canadian subjects (male 14, female 15); average age: 23.3 ± 1.5 years (Belin et al., 2008). Both Japanese and Canadian participants consisted exclusively of undergraduate students.

After a thorough explanation of the study, written informed consent was obtained from all subjects, and the study was approved by the Ethics Committee of Nippon Medical School.

VOICE MATERIALS

The MAVs: 10 French-Canadian actors expressed specific emotional vocalizations and non-emotional vocalizations (neutral sounds) using "ah" sounds. The eight emotional vocalizations were angry, disgusted, fearful, painful, sad, surprised, happy, and pleased. The simple "ah" sounds were used to control the influence of lexical-semantic processing. Since each of the eight emotional vocalizations and the neutral vocalization were spoken by 10 actors, the total number of MAVs sounds was 90. The MAVs are available at: http://vnl.psy.gla.ac.uk/

EVALUATION SCALE

Each emotional vocalization was evaluated using three criteria: perceived emotional Intensity in each of the eight Emotions, perceived Valence, and perceived Arousal. Each scale had a range from 0 to 100.

The Valence scale represented the extent of positive or negative emotion expressed by the vocalization: 0 was extremely negative, and 100 was extremely positive. The Arousal scale represented the extent of excitement expressed by the vocalization: 0 was extremely calm, and 100 was extremely excited. The Intensity scale represented the Intensity of a given emotion expressed by the vocalization: 0 was not at all intense, and 100 was extremely intense. The Intensity scale was used for eight emotions: Anger, Disgust, Fear, Pain, Sadness, Surprise, Happiness, and Pleasure.

METHODS OF EVALUATION BY PARTICIPANTS

The MAVs vocalizations were played on a computer in a pseudo-random order. The subjects listened with headphones at a comfortable hearing level, and they evaluated each emotional vocalization for perceived Intensity, Valence, and Arousal using a visual analog scale in English on a computer (10 ratings per vocalization: 8 Intensity ratings, 1 Valence rating, 1 Arousal rating). Simultaneously, participants were given a printed Japanese translation of the scale labels, and by referring to this Japanese sheet, the test was performed using exactly the same procedure as in the Canadian study (Belin et al., 2008). All Japanese participants performed the experiment using a translation sheet with emotional words translated from English to Japanese. Based on previous studies (Scherer and Wallbott, 1994), the Japanese translation of English emotional labels was independently assessed by three clinical psychologists. Through their discussion, the appropriate emotional labels were determined.

STATISTICAL ANALYSIS

Statistical calculations were made using SPSS (Statistical Package for Social Science) Version 19.0. The Japanese data and the Canadian published data, with permission to verify, were statistically analyzed. A previous study demonstrated gender effects in Canadian participants using the MAV (Belin et al., 2008). Using the same methods to reveal the gender effects, an ANOVA with Emotion, Actor gender, and Participant gender as factors was calculated for ratings by the Japanese listeners. Further, to clarify the cross-cultural effect between Japanese and Canadian participants, three mixed two-way ANOVAs were calculated on ratings of Intensity, Valence, and Arousal. For each mixed ANOVA, to verify the equality of the variance of the differences by Emotions, Mauchly's sphericity was calculated. If the sphericity could not be assumed using Mauchly's test, Greenhouse–Geisser's correction was calculated.

RELIABILITY AND ACCURACY

First, we analyzed the inter-subject reliability of the ratings using Cronbach's alpha. Next, we examined the Intensity ratings for their sensitivity (hit rate, by Emotion) and specificity (correct rejection rate, by rating scale). Based on the previous report (Belin et al., 2008), the accuracy of emotional recognition was investigated using measures of sensitivity (hit rate, by Emotion) and specificity (correct rejection rate, by rating scale). For each vocalization, participants rated the perceived emotional Intensity along each of eight different scales (Anger, Disgust, Fear, Pain, Sadness, Surprise, Happiness, and Pleasure). To calculate sensitivity, for a given portrayed emotion, a maximum Intensity rating in the corresponding scale (i.e., if Intensity rating of Anger was highest when the subject listened to angry vocalization) was taken as a hit; otherwise, as a miss. In other words, emotions with high hit rates are those that